Water Research, Volume 174, May 2020, Article number 115613
DOI:10.1016/j.watres.2020.115613

# Influence of granular activated carbon media properties on natural organic matter and disinfection by-product precursor removal from drinking water

D. M. Golea[1], P. Jarvis[1], B. Jefferson[1], G. Moore[2], S. Sutherland[2], S. A. Parsons[2], S. J. Judd[1*]
[1]Cranfield Water Science Institute, Cranfield University, Bedfordshire, UK.
[2]Scottish Water, Edinburgh, Scotland.
*Corresponding author, s.j.judd@cranfield.ac.uk

## Abstract

Operational and financial constraints challenge effective removal of natural organic matter (NOM), and specifically disinfection by-product (DBP) precursors, at remote and/or small sites. Granular activated carbon (GAC) is a widely used treatment option for such locations, due to its relatively low maintenance and process operational simplicity. However, its efficacy is highly dependent on the media capacity for the organic matter, which in turn depends on the media characteristics.

The influence of GAC media properties on NOM/DBP precursor removal has been studied using a range of established and emerging media using both batch adsorption tests and rapid small-scale column tests. DBP formation propensity (DBPFP) was measured with reference to trihalomethanes (THMs) and haloacetic acids (HAAs). All GAC media showed no selectivity for specific removal of precursors of regulated DBPs; DBP formation was a simple function of residual dissolved organic carbon (DOC) levels.

$UV_{254}$ was found to be a good surrogate measurement of DBPFP for an untreated water source having a high DOC. Due to the much-reduced concentration of DBP precursors, the correlation was significantly poorer for the coagulation/flocculation-pretreateed water source.

Breakthrough curves generated from the microcolumn trials revealed DOC removal and consequent DBP reduction to correlate reasonably well with the prevalence pores in the 5-10 nm range. A 3-6 fold increase in capacity was recorded for a 0.005 to 0.045 $cm^3/g$ change in 5-10 nm-sized pore volume density. No corresponding correlation was evident with other media pore size ranges.

*Keywords: GAC, NOM, pore size, THM, HAA, formation propensity*

# 1 Introduction

Granular activated carbon (GAC) is used extensively in drinking water treatment in various roles, including removal of pesticides, heavy metals and other micro pollutants, and more recently in wastewater reuse (de Almeida Alves et al., 2019, Hoslett et al., 2018; Sun et al., 2018). The process is also frequently applied downstream of conventional coagulation/ clarification for supplementary removal of natural organic matter (NOM) and to improve the bio-stability of the water, through removal of assimilable dissolved organic carbon (DOC) (Bhatnagar and Sillanpää, 2017; Graf et al., 2014; Velten et al., 2011, Liao et al., 2019). It may also be employed at the beginning of the water treatment works (WTWs) as a "roughing" filter to aid with NOM and pesticide removal (Ratnayaka et al., 2008; Reckhow and Singer, 2010; Zeng et al., 2019).

One of the key drivers for NOM removal is the reduction of disinfection by-product (DBP) forming compounds following chemical disinfection (Ndiweni et al., 2019), expressed as the formation propensity (hence DBPFP). The trihalomethanes (THMs) and haloacetic acids (HAAs) have been the most extensively studied DBPs since they are usually present at the highest mass concentration (Gibert et al., 2013; Golea et al., 2017). In the EU, currently only THMs are regulated, with the maximum permissible combined concentration being 100 µg/L. Limits of 80 µg/L or 60 µg/L for 9 or 5 HAAs respectively are currently under consideration in the EU, in alignment with US regulations (USEPA, 2010).

NOM is substantially removed by coagulation/clarification in large-scale potable WTWs, provided rigorous monitoring and control is applied. However, this process is not always appropriate at small scale in remotely located sites where low-maintenance processes are

preferred to reduce labour costs. These include membrane and adsorption technologies, with GAC sometimes favoured on the basis of cost effectiveness and versatility (Bhatnagar and Sillanpää, 2017; Iriarte-Velasco et al., 2008). It is known that the high molecular weight (MW) hydrophobic (HPO) NOM fraction is readily removed by conventional coagulation, such that the influent NOM to GAC processes in secondary potable treatment stages is usually dominated by the low MW and relatively hydrophilic (HPI) fractions (Matilainen et al., 2006). The HPO fraction is generally more reactive with chlorine, with thus a high DBPFP (Golea et al., 2017). When GAC is used as a roughing filter, the main loading of NOM is from HPO and high MW organic compounds. In this case, high MW NOM can block the pores of the adsorbent, preventing other compounds from accessing the adsorbent. The NOM characteristics and the corresponding required GAC media properties are thus influenced by the position of the adsorption process in the treatment scheme (Valdivia-Garcia et al., 2016).

One of the most significant GAC media properties is pore size ($d_p$) distribution; the useful pore size range for NOM has been shown to be the secondary micropores (1-2 nm) and the mesopores (2-50 nm), with pores smaller than 1 nm offering negligible adsorption (Dastgheib et al., 2004; Velten et al., 2011). High MW (1-10 kDa) NOM such as humic substances with molecular diameters above 2 nm are adsorbed largely within the mesopores. However, adsorption is not solely governed by bulk physical properties, since physicochemical properties – and specifically surface charge and hydrophobicity – also impact on adsorption; HPO NOM is preferentially removed over hydrophilic material. It thus follows that the low MW hydrophilic fraction, whilst less reactive with chlorine, poses the greatest challenge to

74 removal by GAC and may still have a sufficiently high DBPFP to be problematic (Golea et
75 al, 2017).

76 Given the above challenge presented by NOM removal by GAC it is of interest to determine
77 (a) the most effective GAC media for DBP precursor removal from different water sources
78 and (b) the most effective position of the GAC process in the treatment train. Previous studies
79 of GAC adsorption of NOM have tended to focus on physicochemical characteristics of the
80 NOM, rather than those of the GAC (Aschermann et al, 2018; Shimabuku et al, 2017; Velten
81 et al, 2011), with this work including the key area of competitive adsorption/desorption of
82 NOM and micropollutants (Aschermann et al, 2018; Piai et al, 2019). However, there have
83 thus far been few studies quantitatively correlating NOM or DBPFP adsorption with media
84 characteristics. Those studies that have encompassed GAC media with a range of pore sizes
85 (Gui et al, 2018) have not quantitatively correlated media capacity with pore-related
86 parameters.

87 The current study correlates GAC properties, specifically the media pore size distribution,
88 with NOM and DBPFP removal from two water sources having differing NOM chemistry
89 with reference to DBPFP. Tests encompassed both batch adsorption measurements and small-
90 scale media column tests for determining adsorption capacity, and DBPFP both as
91 trihalomethanes (THMFP) and haloacetic acids (HAAFP). Outcomes can then be expected to
92 (i) inform decisions regarding GAC media selection for NOM removal, and (ii) direct
93 developments on novel adsorptive media for maximum NOM capacity.

# 2 Methods and materials

## 2.1 Sampling

Source water was taken from two WTWs of differing process configuration (Fig. 1). WTW A employs simple media filtration via a pressurised sand filter (PSF) followed by GAC adsorption. WTW B uses clarification by conventional coagulation-flocculation followed by dissolved air flotation (DAF), rapid gravity filtration (RGF) and GAC adsorption. The water used in the current study was sampled from the filtrate, i.e. downstream of the PSF stage at the WTW A site (*Water A*) and the RGFs at WTW B (*Water B*).

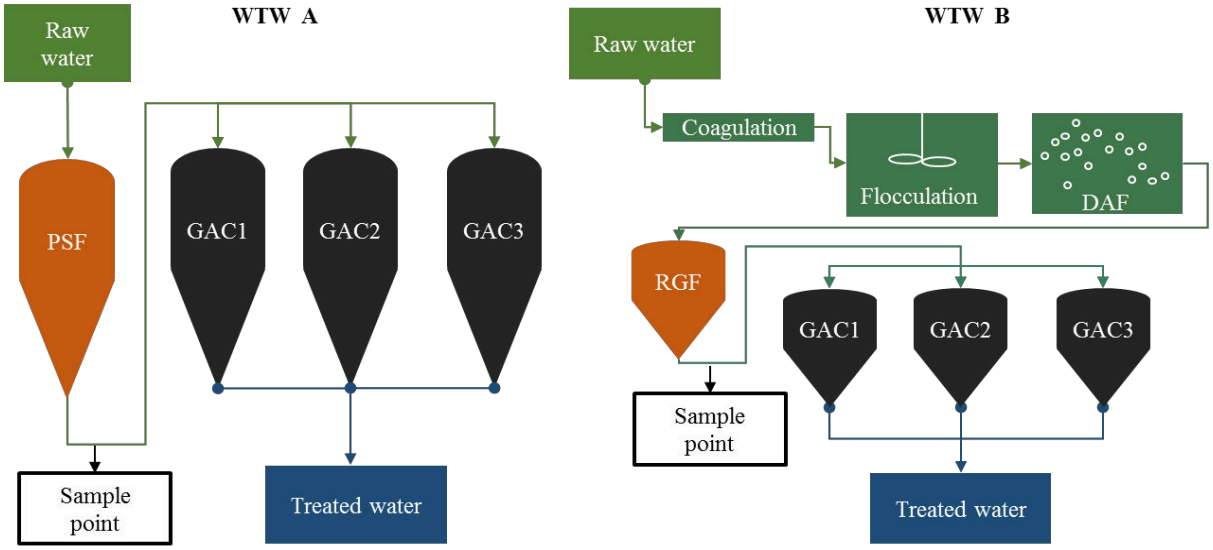


Figure 1. Water treatment flow sheet at the 2 WTWs featuring rudimentary and advanced pretreatment respectively. WTW A: Pressure sand filtration; WTW B: Coagulation/flocculation, dissolved air flotation and rapid gravity filtration.

## 2.2 GAC media

GAC media sourced from four different precursor materials were used, selected to encompass a range of specific surface areas and $d_p$ values, and comprised:

- Bituminous coal: *COL-L900* (Carbon-Activated LTD, Bristol, UK); *Filtrasorb F400* (Chemviron, Tipton, UK).
- Coal: *208 EA* (Chemviron); *Hydraffin XC30* (Donau Carbon, Frankfurt, Germany).
- Coconut shell: *DEO*, *HT5* (Eurocarb, Bristol, UK); *FY5* (CPL Carbon Link, Wigan, UK))
- Bovine bones: *Brimac* (Inverclyde, UK).

## 2.3 GAC preparation

For the batch adsorption isotherm tests, the GAC media was crushed and fractionated by sieving to generate a 38-90 µm size fraction. The media were then washed thoroughly in ultrapure water, dried overnight at 105°C and kept in a desiccator until use for the adsorption capacity batch tests. For the rapid small-scale column test (RSSCT), the GAC was crushed using a hammer mill, and then sieved to between 212 and 300 µm, yielding a column diameter:grain size ratio of >30:1 and so avoid channelling effects. The media were then then rinsed and dried as with the isotherm tests (Philippe et al., 2010), then re-wetted prior to testing by boiling in DI water for 10 minutes. Media preparation in this manner has been shown to have no significant impact on the internal structural pore features (Ando et al., 2010).

## 2.4 GAC characterisation using $N_2$ pore size distribution

The total pore volume $V_{total}$ of the dried media was measured as the adsorbed volume of $N_2$ gas near the saturation volume ($P/P_0$=0.98) (Iriarte-Velasco et al., 2008), and the surface area calculated from Brunauer–Emmett–Teller (BET) theory (Brunauer et al., 1938). The $d_p$ distribution was determined using density functional theory (DFT) for pores sizes quantified between 0.7 and 36 nm (Velten et al., 2011). The DFT model was employed to provide a

more accurate interpretation of the isotherm data for non-homogenous liquids on microporous materials (Lastoskie et al., 1993). Calculations assumed a graphite structure with slit-like pore geometry (Iriarte-Velasco et al., 2008; Moore et al., 2001) using an *ASAP 2010* (Micrometrics, St Andrews, UK) physisorption apparatus. GAC were primarily characterised by the volume of the secondary micropores (1-2 nm) and mesopores (2-50 nm), since smaller pores have been shown to exhibit negligible adsorption of NOM (Velten et al., 2011). Further analysis of the $d_p$ distribution was undertaken to correlate specific pore size ranges with removal of NOM, with a maximum measured pore size of 30 nm.

## 2.5 Adsorption capacity batch tests

The prepared media were dosed at 0-0.1 g/L, with dose modulated based on the DOC of the source water, and agitated continuously in an orbital shaker at 200 rpm for 24 hours at 20°C, which preliminary trials established was a sufficient period for equilibration. The water samples were then 0.45 µm-filtered prior to analysis. The equilibrium adsorption capacity ($q_e$, mg DOC/g adsorbent) was calculated as the change in solution DOC concentration $C_i$ – $C_e$, $C_i$ being the initial and $C_e$ the equilibrium concentration, divided by the adsorbent concentration $D_o$. Base $D_o$ values of 150 and 50 mg/L for *Water A* and *B* respectively were established as being appropriate for removing significant organic matter whilst still leaving a sufficient (>1 mg/L) residual DOC concentration to permit subsequent THMFP and HAAFP analysis. All tests were carried out in duplicate.

## 2.6 Rapid small-scale column tests

1000 L samples of water were taken from WTW A and B and were passed through media beds of 15 mm diameter and 140 mm height for 14 days. The RSSCT columns were

undertaken according to the recommendations of Crittenden et al. (2012), following the proportional intra-particle diffusivity (PD) model:

$$\frac{EBCT_{SC}}{EBCT_{LC}} = \frac{d_{G,SC}}{d_{G,LC}} = \frac{t_{SC}}{t_{LC}} \quad \text{Equation 1}$$

$$M_{SC} = EBCT_{LC} \times \frac{d_{p,SC}}{d_{p,LC}} \times Q_{SC} \times \rho_{LC} \quad \text{Equation 2}$$

Where $EBCT_{LC}$ = empty bed contact time in full-scale adsorber; $EBCT_{SC}$ = empty bed contact time for small experimental columns; $d_{G,SC}$ = diameter of GAC particles in small column; $d_{G,LC}$ = diameter of GAC particles in full scale column; $t_{SC}/t_{FS}$ = time required to conduct a small-scale test ($t_{SC}$) relative to the time necessary to conduct a large-scale test ($t_{FS}$); $M_{SC}$ = the mass of media in the small column; $Q_{SC}$ = the flow in the small column; $\rho_{LC}$ = density of the GAC media in the large column. Equation 2 was used to ensure that the different GAC media densities were accounted for.

For NOM removal, the PD approach has proven to work well since the relatively high MW organic matter diffuses significantly faster into the pores of the GAC when compared to micropollutants (Summers et al., 1995). Scaled from an operational empty bed contact time of 20 minutes for full scale adsorbers as typically used in Scottish Water ($EBCT_{LC}$), this translated to an EBCT in the experimental columns ($EBCT_{SC}$) of 4.24 minutes for a 25 mL bed volume.

## 2.7 Sample chlorination and DBP formation potential determination

250 mL water samples were diluted to a concentration of 1 mg C/L and buffered to pH 7 and dosed with NaOCl at a $Cl_2$:DOC weight ratio of 5:1. Samples were then sealed and stored in the dark at a temperature of 25°C for seven days. The chlorine was then quenched with

excess sodium thiosulphate and the THM and HAA concentrations measured. The total THM concentration (tTHM) was measured using gas chromatography spectrometry with headspace injection using the standard USEPA 551 method (USEPA, 1998). The total concentration of the five most predominant HAAs ($tHAA_5$) was measured using liquid-liquid separation and analysis by gas chromatography with mass spectrometric detection following the USEPA method 552.3 (APHA, 2012), with at least seven injections undertaken for each measurement.

# 3 Results and discussion

## 3.1 Source water characterisation

Sample filtrate water quality varied significantly between the two sites (Table 1) due to the differences in pre-treatment, *Water B* samples receiving full clarification whereas *Water A* which was treated only by sand filtration (Fig. 1). Whilst the pH and conductivity values were both lower for the *Water A* samples (6.8 and 166 µS/cm, cf. 8.1 and 569 µS/cm for *Water B*), reflecting the reduced chemical addition, the DOC of *Water A* was double that of *Water B* and the $UV_{254}$ absorption 3.8 times higher. $UV_{254}$ absorption is recognised as broadly reflecting the HPO content of the water (Bhatnagar and Sillanpää, 2017), which was commensurately 3.4 times higher for *Water A*. Conversely, the HPI content was 2.8 times lower. The elevated DOC and HPO concentrations of *Water A* were reflected in THMFP and $HAA_5FP$ values, respectively 1.25 and 4.2 times higher on average for *Water A* cf. *Water B*. These factors increased to 2.4 and 8 respectively under worst-case conditions. No significant change in the distribution of individual DBP species was observed between the two samples, with trichloromethane being the predominant THM (85-90% by weight) and the

dichloroacetic and trichloroacetic acids making up 80-85% of the $tHAA_5$ concentration in both cases.

**Table 1:** Physicochemical characteristics of the two different water sources.

| *Parameter* | *Water A* | *Water B* |
|---|---|---|
| pH | 6.8 | 8.1 |
| DOC (mg/L) | 5.98 | 3.12 |
| $UV_{254}$ (/cm) | 0.254 | 0.068 |
| SUVA (mg/L/m) | 4.25 | 2.18 |
| tTHM (µg/L) | 676.3 | 282 |
| THMFP (µg/L per mg DOC) | 113.1 | 90.4 |
| tHAA (µg /L) | 1006.4 | 126 |
| $HAA_5FP$ (µg/L per mg DOC) | 168.3 | 40.4 |
| Colour (mg/L Pt/Co) | 33 | 4.47 |
| Turbidity (NTU) | 0.37 | 0.1 |
| Conductivity (µS/cm) | 166 | 569 |
| HPO (mg/L) | 3.44 | 1 |
| TPI (mg/L) | 1.25 | 0.71 |
| HPI (mg/L) | 0.37 | 1.05 |

## 3.2 Physical media characteristics

Total pore volumes ranged from 0.331 (*DEO*) up to 0.581 $cm^3/g$ (*HT5*) for the GAC media investigated. Mesopore volumes measured for the GAC media studied ranged from as low as 0.004 $cm^3/g$ (*FY5*) up to 0.156 $cm^3/g$ (*XC30*). The secondary micropores were between 0.174 $cm^3/g$ (*DEO*) and 0.401 $cm^3/g$ (*HT5*) (Table 2). None of the media had $d_p$ values above 27.3

214 nm. The media with the highest total pore volume (*HT5*) had pores that were predominantly
215 in the 1-2 nm pore size range (0.401 $cm^3/g$). The media with the most evenly distributed pore
216 sizes was the coal media *XC30* with 0.205 (57%) and 0.156 (43%) $cm^3/g$ distributed between
217 micro and mesopores respectively (Fig 2). *F400* had a 78:22 distribution of pore volume
218 between the micropore and mesopore size range. Further examination revealed pore size to be
219 predominantly below 5 nm, contributing 84.0-99.9% of the total pore volume (Fig 2). The
220 media with the highest proportion of small pores (<5) nm were the coconut shell media (*FY5*
221 and DEO) at 99.8 and 99.9%. Conversely, the GAC with the smallest proportion of small
222 pores were the coal-based *XC30* and the bone char media *Brimac*, at 83.9 and 85.7%
223 respectively.

224 There was good agreement between the specific surface area values measured in the current
225 study ($S_{BET}$) and those reported by the supplier ($S_{BET,s}$) and other researchers (Table 2). The
226 exception was the $S_{BET}$ for *Brimac* (bone char). For *Brimac*, $S_{BET}$ has been previously reported
227 as being 130-283 $m^2/g$, with a $V_{total}$ of 0.287 $cm^3/g$ (Moreno et al., 2010; Nili-Ahmadabadi,
228 2011), compared to the much higher values of 841 $m^2/g$ and 0.430$cm^3/g$ respectively
229 recorded in the current study. For *F400*, there was a small difference in the $V_{micropores}$
230 measured in the current study (0.271 $cm^3/g$), a value which was 20-33% lower than the 0.30-
231 0.41 $cm^3/g$ range previously reported (Summers et al., 2010, Dastgheib et al., 2004, and
232 Gibert et al., 2013, Table 2). Differences are likely to reflect the media sample heterogeneity,
233 a point noted by other researchers (Ando et al., 2010) and differences in the range of pore
234 sizes quantified during the analysis. The surface area of the *Brimac* media was nonetheless
235 the lowest measured of all those investigated.

**Table 2:** The physicochemical properties of the media used for removal of NOM from two different water sources.

| ***GAC media*** | $V_{total}$ [1] cm³/g | $d_p$ nm | $V_{micropores}$ [2] cm³/g | $V_{meso-pores}$ [3] cm³/g | ***DFT area ($m^2/g$)*** [4] 0.7-1.7 | 1-2 | >2 | *Granulation* [5] mm | $S_{BET,s}$ [5] m²/g | $S_{BET}$ m²/g | ***IN*** [5,6] mg/g | *Precursor* [5] |
|---|---|---|---|---|---|---|---|---|---|---|---|---|
| *COL-L900* | 0.460 | ≤26.1 | 0.347 | 0.112 | 444 | 506 | 72 | 0.425-1.70 | 900-1000 | 977±5 | 900 | Bituminous coal |
| *F400* | 0.442 | ≤26.1 | 0.271 | 0.073 | 431 | 416 | 49 | 0.425-1.70 | 1050 | 1032±5 | 1050 | Bituminous coal |
| *208EA* | 0.517 | ≤16.1 | 0.301 | 0.120 | 424 | 465 | 67 | 0.6-1.7 | 1000 | 1078±6 | 1000 | Coal |
| *XC30* | 0.511 | ≤26.1 | 0.205 | 0.156 | 325 | 340 | 66 | 0.6-2.36 | 1000 | 986±6 | 950 | Coal |
| *DEO* | 0.331 | ≤27.3 | 0.174 | 0.013 | 274 | 285 | 8 | 0.6-1.70 | 800 | 809±11 | 825 | Coconut shell |
| *HT5* | 0.581 | ≤27.3 | 0.401 | 0.029 | 621 | 652 | 14 | 0.42-1.70 | 1400 | 1419±12 | 1300 | Coconut shell |
| *FY5* | 0.400 | ≤16.1 | 0.288 | 0.004 | 452 | 471 | 3 | 1.40-3.35 | 1150 | 1043±11 | 1100 | Coconut shell |
| *Brimac* | 0.430 | ≤25 | 0.246 | 0.131 | 334 | 373 | 62 | 0.7-2.38 | 200 | 841±3 | 700 | Bovine bones |

[1]According to DFT (density functional theory), determined to <30nm; [2]1-2 nm pore size range; [3]>2 nm pore size; [4]with reference to pore size range indicated; [5]Data sourced from supplier technical sheets; [6]Iodine number.

**Table 3:** Volumetric pore size distribution, determined from DFT for pores sizes <30 nm.

| *Media/pore size:* | ***<0.7nm*** | ***0.7-5nm*** | ***5-10nm*** | ***10-15nm*** | ***15-20nm*** | ***20-25nm*** | ***25-30nm*** | ***Total*** |
|---|---|---|---|---|---|---|---|---|
| *Col-L900* | 0.001 | 0.440 | 0.011 | 0.006 | 0.002 | 0.001 | 0 | 0.460 |
| *F400* | 0.055 | 0.375 | 0.010 | 0.002 | 0 | 0 | 0 | 0.442 |
| *208EA* | 0.096 | 0.386 | 0.027 | 0.008 | 0.001 | 0 | 0 | 0.517 |
| *XC30* | 0.115 | 0.314 | 0.042 | 0.018 | 0.012 | 0.009 | 0.001 | 0.511 |
| *DEO* | 0.144 | 0.183 | 0.001 | 0.002 | 0.000 | 0 | 0 | 0.331 |
| *HT5* | 0.151 | 0.417 | 0.005 | 0.004 | 0.003 | 0.002 | 0 | 0.581 |
| *FY5* | 0.108 | 0.291 | 0 | 0.001 | 0 | 0 | 0 | 0.400 |
| *Brimac* | 0.053 | 0.316 | 0.029 | 0.016 | 0.010 | 0.007 | 0 | 0.430 |

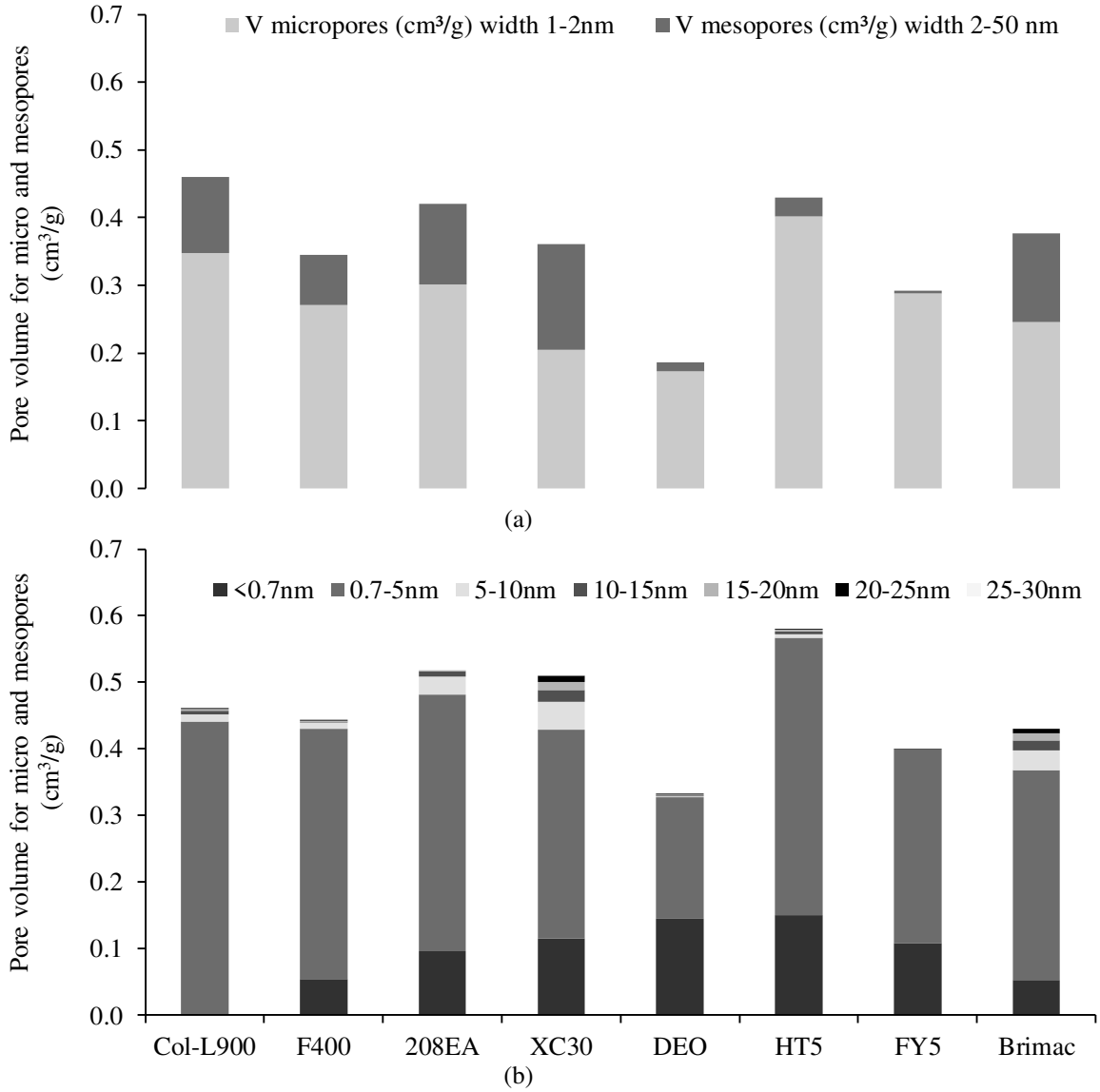


Figure 2. GAC pore volumes for (a) the micro (1-2 nm) and mesopores (2-50 nm) pore size, and (b) the full distribution of pore sizes.

## 3.3 Batch adsorption isotherms

Batch adsorption isotherms revealed significant differences in DOC capacity across the different media (Fig. 3), with *DEO* having the lowest capacity (1.19 and 1.76 mg/g for *Waters A* and *B* respectively) and *XC30* the largest (20.7 and 27.1 mg/g respectively).

The higher capacity for the *Water B* organic matter reflects the impact of the coagulation pre-treatment on the DOC characteristics, which similarly accounts for the difference in THMFP. Increased GAC capacity following coagulation has been noted by Karanfil et al. (1999), and was attributed to the removal of high MW HPO NOM which otherwise cause pore blockage and so reduce media capacity. Two-fold changes in THMFP between raw and treated waters have been previously reported for predominantly upland water samples (Golea et al, 2017).

No selective removal of THM precursors was observed for any of the media, the THMFP values all lying between 100 and 113 µg THM / mg DOC for *Water A* and 75-83 for *Water B* (Fig. 4a), despite a >10 times change in capacity. THMFP tended to decrease with increasing media capacity regardless of the media characteristics, a trend more readily recognisable from the non-normalised THM concentration data (Fig. 4b). However, no other trend in THM concentration vs bulk media characteristics, specifically *IN* and $S_{BET}$, was evident.

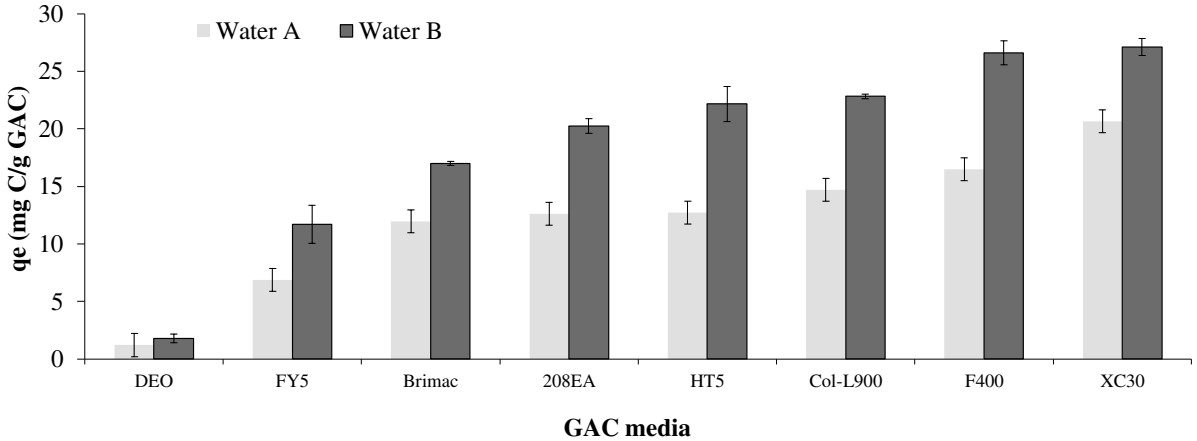


Figure 3. Organic carbon capacity ($q_e$) of the 8 media.

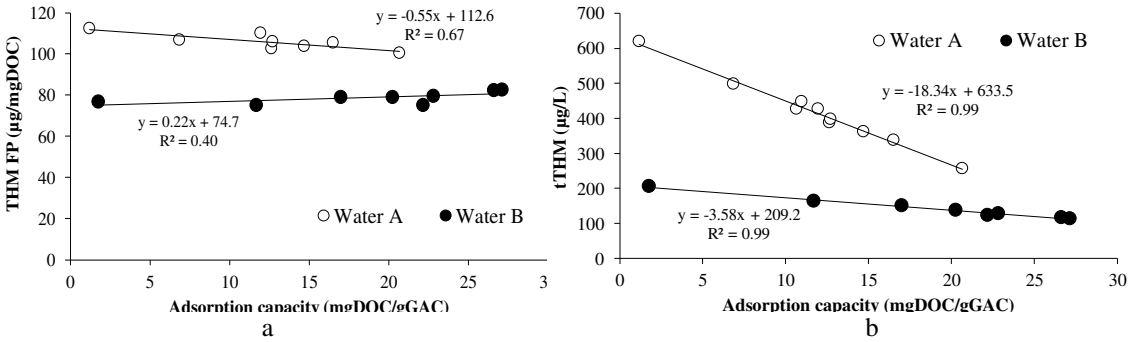


Figure 4. (a) Normalised THMFP and (b) tTHMs for *Waters A* and *B*. Each datum corresponds to a single GAC media.

## 3.4 Rapid small-scale column tests

The breakthrough curves for the individual media inferred relative capacities which generally followed the trends recorded for the batch tests (Fig. 5). Breakthrough curves were steeper for *Water A* due to the higher organic loading for this source water and the impact of the larger and HPO organic carbon fraction exhausting the GAC surface area.

Overall, the two coal-based media (*208EA* and *XC30*) offered the highest capacities, reflected in shallower breakthrough curves. For *Water A*, the DOC removal efficiency for these media progressively decreased from 92-94% to 25-27% after 22,000 BVs (Fig. 5a), the maximum volume reached for this campaign. For *Water B*, *XC30* provided the shallowest curve, from 92% DOC removal initially to an end value of 50%, with two other coal-based media (*F400* and *208EA*) removing 90-91% DOC initially and progressively declining to 36-38%.

Differences in performance between *Waters A* and *B* again reflect the impact of clarification pre-treatment, which both decreases the DOC concentration and the proportion of the high MW organic compounds which otherwise block the media pores.

The lower MW NOM fraction, reported to be in the 0.5-5 nm size range (Dastgheib et al., 2004; Karanfil et al., 1999; Moore et al., 2001; Velten et al., 2011) can then access the media pores (Graf et al., 2014; Iriarte-Velasco et al., 2008) with the 2-50 nm mesopores expected to provide the most accessible adsorption sites for such NOM macromolecules. This was consistent with the two media having the lowest mesopore volumes (*FY5* and *DEO*, derived from coconut shell, with mesopore volumes of 0.004-0.013 $cm^3/g$) offering the lowest DOC removal (Fig. 5b) despite their relatively high surface area ($S_{BET}$ values). Conversely, the mesopore volume of the *208EA* and *XC30* media were amongst the highest of those tested. The *Brimac* media performed comparatively well for both water sources despite its low $S_{BET}$ value due to its high mesopore volume.

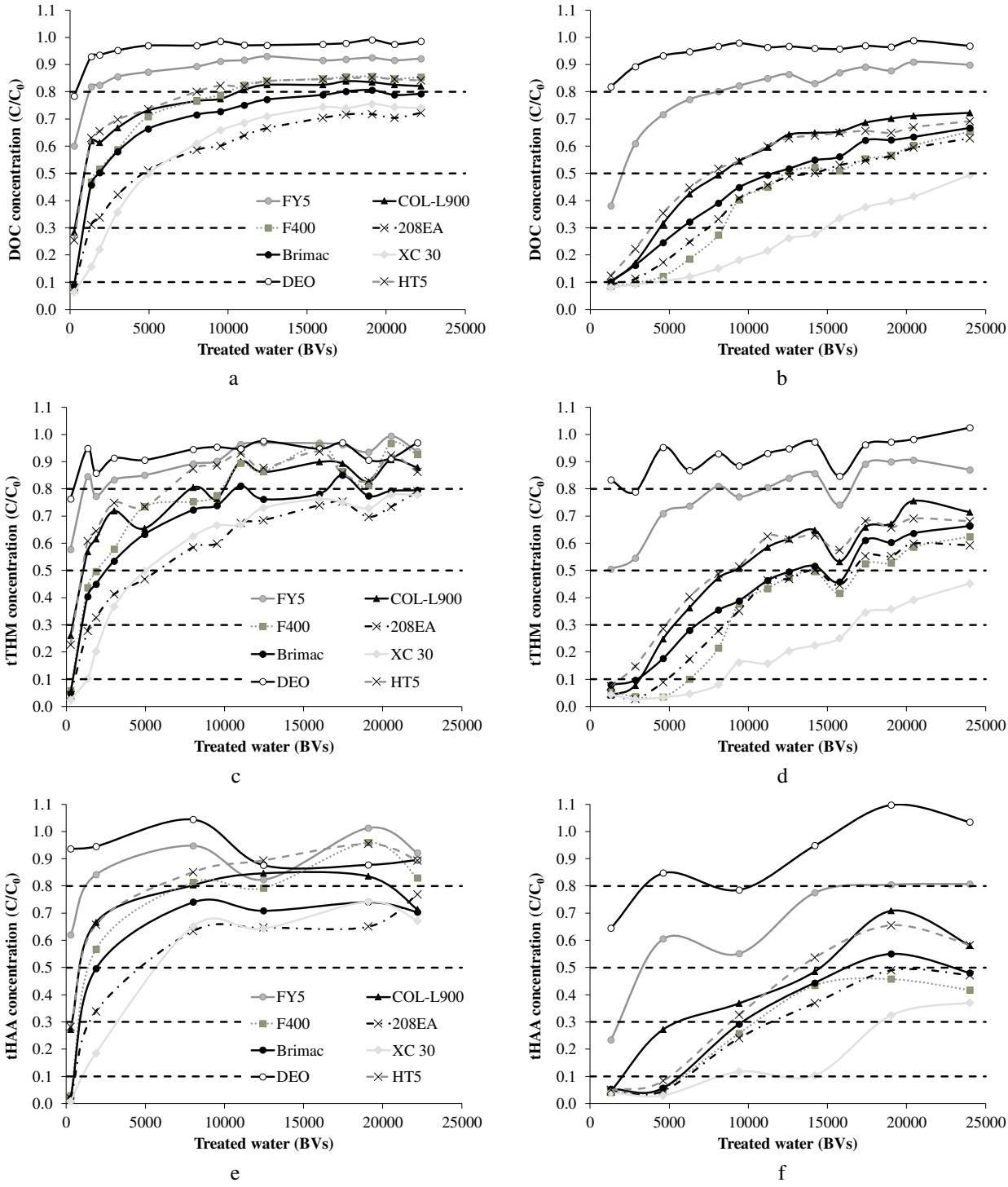


308 Figure 5. Removal of (a-b) DOC and precursors of (c-d) tTHM and (e-f) tHAA for waters *A* (a, c, e)
309 and *B* (b, d, f), for up to 24,000 bed volumes (BVs) of treated water.

310

311 The reduction in THMFP (Figure 5c-d) and HAAs (Figure 4e-f) generally followed the
312 removal profile of the DOC. There was no indication of selective removal of DBP
313 precursors from either water by any of the GAC media, a result consistent with that
314 observed from the batch experiments.

315 The throughput to 30, 50 and 80% breakthrough ($BV_{30}$, $BV_{50}$ and $BV_{80}$) of DOC (Table
316 4) confirm *XC30* as achieving the highest $BV_{30}$ for both water sources. For *Water A*,
317 *XC30* treated almost double the amount of water (2514 BVs) than the next best GAC
318 (*208EA*), and respectively three and seven times more water than *Brimac* and the best
319 coconut shell-based media *HT5*. The *Brimac* GAC performed at a similar level to the
320 *F400* media. Both *FY5* and *DEO* failed to achieve a quantifiable $BV_{30}$ due to rapid
321 exhaustion at <267 BVs, the point when the first sample was taken. The same order of
322 removal was seen when the $BV_{50}$ was considered, although the differences were less
323 pronounced, with the best performing media being *XC30* with a $BV_{50}$ of 5059 compared
324 with only 946 BVs for *HT5*. The $BV_{80}$ indicated more significant differences between
325 the media, with no $BV_{80}$ value obtained after 23,980 BVs for two of the media (*XC30*
326 and *208EA*) for *Water A* indicating removal was always >20%. This compares with a
327 $BV_{80}$ of only 503 for *DEO*. For the other GAC, *Brimac* treated 40% more water than
328 *F400*, while *COL-L900* treated the same number of BVs as *HT5* (946).
329

**Table 4:** Throughput to a filtrate DOC of 30%, 50% and 80% of the feed concentration ($BV_{30}$, $BV_{50}$ and $BV_{80}$ respectively) for the GAC media studied by RSSCT, waters *A* and *B*, $EBCT_{LC}$ = 20 minutes.

| GAC media | WTW A | | | WTW B | | |
|---|---|---|---|---|---|---|
| | $BV_{30}$ | $BV_{50}$ | $BV_{80}$ | $BV_{30}$ | $BV_{50}$ | $BV_{80}$ |
| ***COL-L900*** | 355 | 946 | 10,710 | 4,467 | 8,284 | >>23,980 |
| ***F400*** | 858 | 1,775 | 10,030 | 8,402 | 12,308 | >>23,980 |
| ***208EA*** | 1,301 | 4,704 | >>22,194 | 7,455 | 13,728 | >>23,980 |
| ***XC30*** | 2,514 | 5,059 | >>22,194 | 14,911 | 23,964 | >>23,980 |
| ***DEO*** | <<267 | <<267 | 503 | <<1,302 | <<1,302 | 1,302 |
| ***HT5*** | 355 | 946 | 8,047 | 3,875 | 7,633 | >>23,980 |
| ***FY5*** | <<267 | <<267 | 1,242 | <<1,302 | 2,041 | 8,284 |
| ***Brimac*** | 858 | 1,775 | 17,101 | 5,798 | 11,657 | >>23,980 |

For *Water B*, *XC30* was again the best performing media with a $BV_{30}$ of 14,911, a value substantially higher than the next best GAC *F400*, having a $BV_{30}$ of 8,402. No $BV_{30}$ value was recorded for *DEO* and *FY5* since the 30% target was exceeded before the first sample taken at 1,302 BVs. This was also the case for the $BV_{50}$ value for *DEO*, whereas the corresponding value for *FY5* was 2,041. This value was less than 10% of the $BV_{50}$ values recorded for *XC30*. All media other than *FY5* and *DEO* removal achieved removal exceeding 20% throughout the run, thus providing no measurable $BV_{80}$, with *XC30* maintaining ≥50% removal.

## 3.5 $UV_{254}$ for monitoring of DBP formation propensity breakthrough

It is of practical significance to correlate DBP breakthrough with a more readily monitored water quality determinant, such as $UV_{254}$ absorbance. $UV_{254}$ is widely acknowledged as being a reasonable analogue measurement for DBPFP due to its association with the more labile HPO organic content of the NOM (Bougeard et al., 2010; Karapinar et al., 2014). Breakthrough data based on number of BVs passed

recorded for 10, 30 and 50% breakthrough ($BV_{10}$, $BV_{30}$, and $BV_{50}$ respectively) for *Waters A* and *B* (Fig. 6) indicate a consistently better correlation for the former. $R^2$ values range from 0.98 to 1.00 for *Water A* data, compared with 0.75-0.99 for *Water B*. This is a consequence of the increased HPO content of the DOC in *Water A* compared with *Water B*, which was subject to pre-clarification. Similar increases in DBPFP data scatter for residual DOC following clarification have been reported by Golea et al (2017).

However, the slope for these correlations varies significantly across the different data sets, from 0.99 to 1.36 for *Water A* and 0.52-1.09 for *Water B* with no pattern evident. This may reflect the vagarious nature of the reactivity of the organic carbon, as noted by previous authors (de la Rubia et al, 2008; Golea et al, 2017). Thus, whilst $UV_{254}$ provides a reasonable representation of DBPFP for both raw and treated waters, and is apparently unaffected by the GAC media characteristics, the coefficient is dependent on the DOC characteristics.

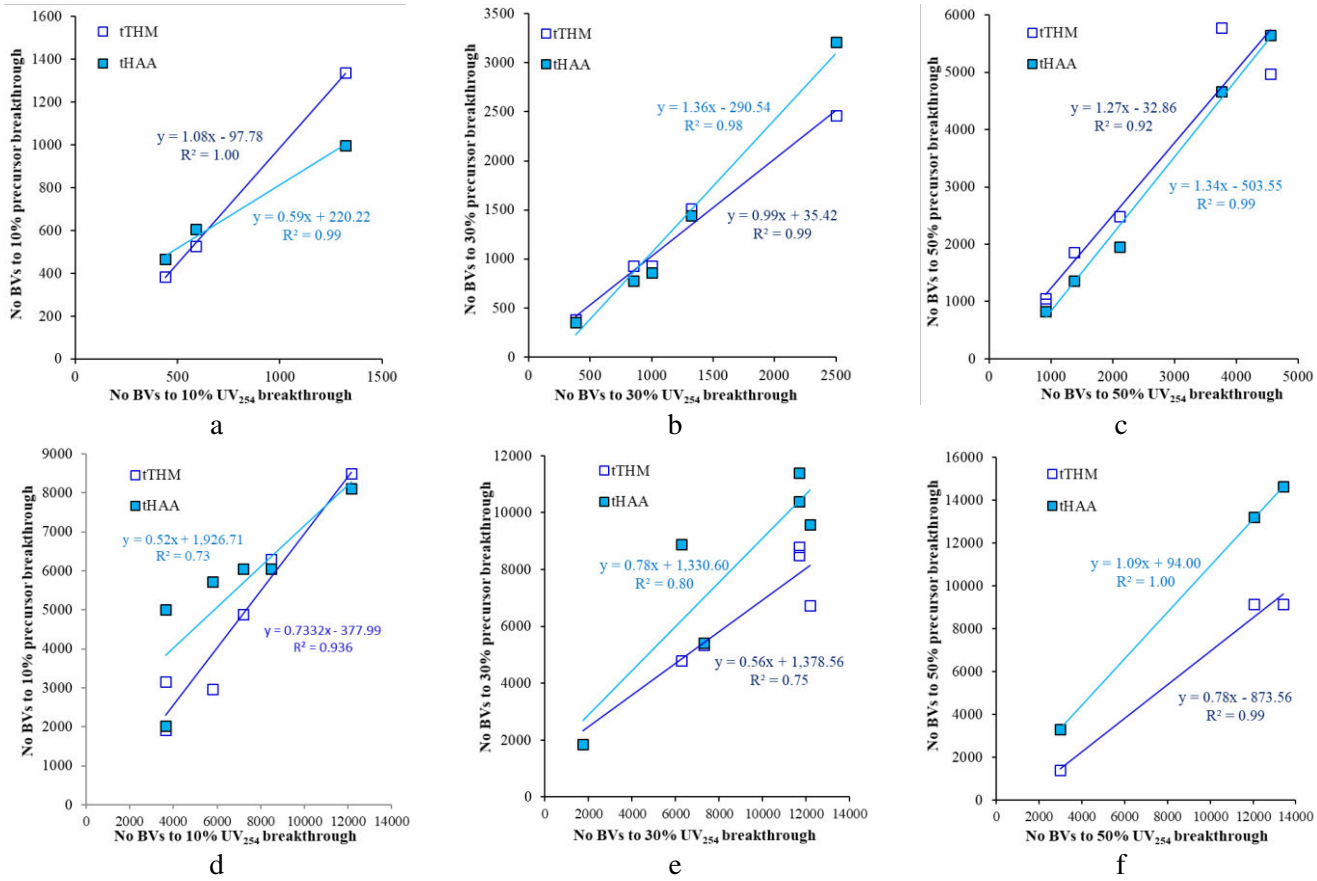


Figure 6. Correlation of bed volumes passed until target percentage breakthrough is reached, DBP precursor concentration vs. $UV_{254}$ for waters *A* (a-c) and *B* (d-f) at 10% (a, d), 30% (b, e) and 50% (c, f) breakthrough. For a single correlation each individual datum relates to a single GAC media.

## 3.6 Correlation of DOC removal with GAC characteristics

A consideration of the impact of media characteristics on the removal of DOC and THMFP from the RSSCTs (Fig. 7) indicates a reasonable correlation of the $BV_{30}$ and $BV_{50}$ data for both DOC and tTHM concentration with the absolute pore volume density for the 5-10 nm pore size range $V_{p,5\text{-}10}$ (Fig. 7a-b). The tHAA breakthrough data also correlated reasonably with this pore size range (Fig. 7c). Across these 12 data sets $R^2$ values ranged from 0.59 to 0.83 for all but the $BV_{30}$ data set for tTHM breakthrough, for

379 which there was no evident correlation ($R^2$ = 0.20). Against this, all correlations
380 between the breakthrough BV and pore volume density produced for the other pore size
381 ranges generated $R^2$ values below 0.27 (Supplementary Information, Table S1).
382 Evidence therefore suggests that removal of NOM-derived DOC, and subsequently the
383 THM and HAA byproducts generated from the residual DOC in the treated water, is
384 primarily a function of the density of 5-10 nm-sized pores in the GAC media. This is a
385 result consistent with that of Velten et al (2011), who advocated selection of 1-50 nm
386 pore-sized GAC media for NOM removal. The present research suggests that the key
387 pore size range to be 5-10 nm.

388

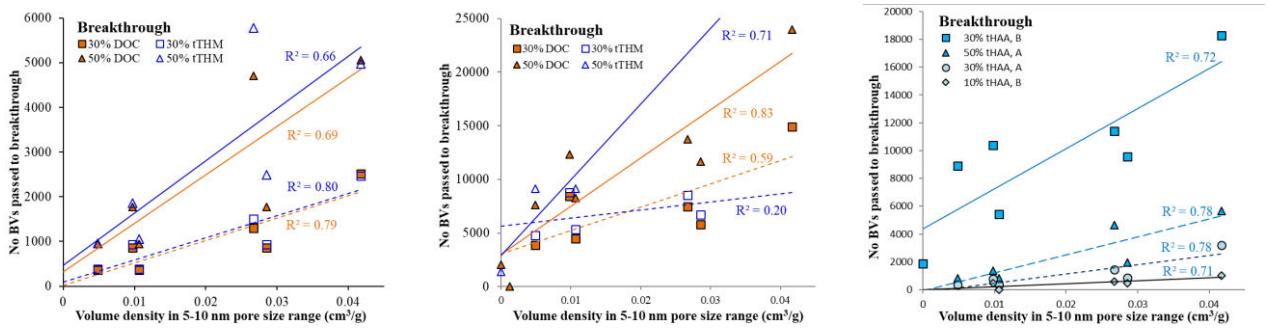


389
390 Figure 7. No. BVs passed to 30% and 50% breakthrough of DOC and tTHMs vs. total volume of pores
391 within 5-10 nm size range for waters (a) *A*, and (b) *B*, and for (c) 10-50% breakthrough of
392 tHAAs.

393

394 The values of the slopes depicted in Figure 7, i.e. $\Delta BV_{breakthrough}/\Delta V_{p,5\text{-}10}$, provide an
395 indication of the extent to which the practical adsorption capacity of the media is
396 influenced by the 5-10 nm pore volume. Accordingly, in the case of *Water A* (Fig. 8),
397 the volume treated to 50% breakthrough increases by 105-125 BVs per $cm^3$/kg 5-10nm

pore volume density based on either DOC or DBPFP concentration. The corresponding range for *Water B*, for an organic carbon concentration around half that of *Water A*, is 500-670 BVs per $cm^3$/kg – the difference being attributable to the pore-blocking effect of the HPO in *Water A*. In both cases, the tHAA data forms the top of the range.

There is evidently a significant influence of the total 5-10 nm pore volume per kg material on the media capacity; 3-6 fold capacity changes arise, the precise value depending on the % breakthrough value, as $V_{p,5\text{-}10}$ changes from 0.005 to 0.042 $cm^3$/g. Whilst previous authors have qualitiatively identified the importance of pores above 3 nm in size, specifically for removing humic and fulvic acid-like substances (Gui et al, 2018), the quantification of practical capacity in terms of breakthrough volume against the total volume provided by pores within a specific size range has not previously been reported.

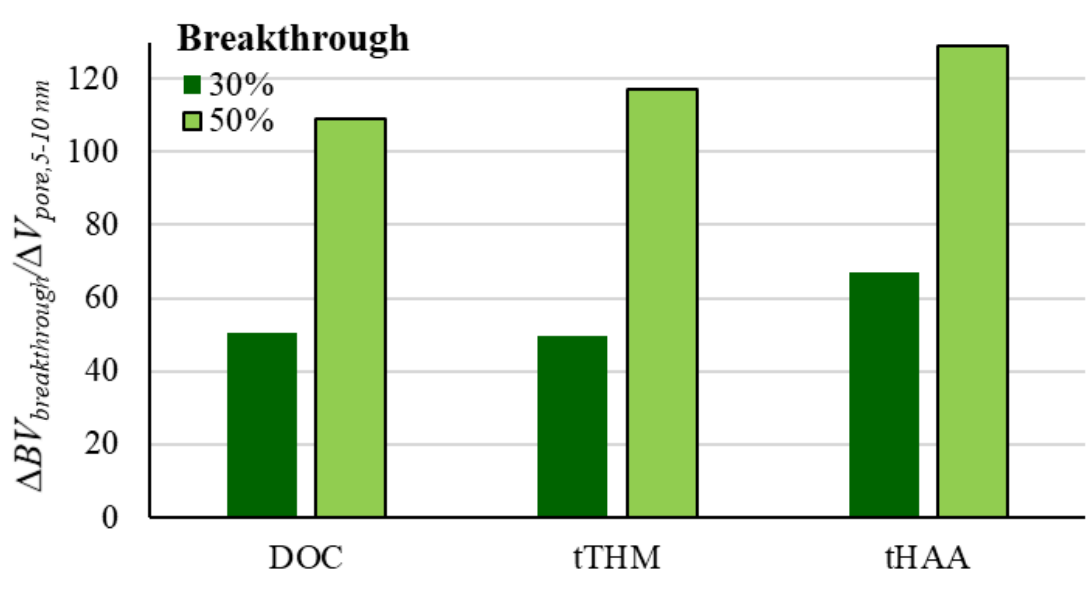


Figure 8. Values of slopes in Fig. 7a and c, i.e. the change in treated volume to breakthrough as a function of the volume of pores in the 5-10 µm size range ($\Delta BV_{breakthrough}/\Delta V_{p,5\text{-}10}$) in units of BV per $cm^3$/kg, for *Water A*.

Results are comparable with previous work on NOM removal by GAC, with relatively low water volumes treated prior to significant breakthrough (e.g. 50% DOC breakthrough at 5-10,000 BVs for the treatment of water containing ~1 mg/L of DOC (Li et al., 2007; Velten et al., 2011). In comparison, removal of micropollutants normally provides higher removal levels for more sustained periods (e.g. 80% removal of the antibiotic sulfamethoxazole after ~68,000 BVs, Greiner et al., 2018). In the current study most of the media removed 20-30% DOC after extended run times for both water sources, with the most effective media removing >50% DOC after >20,000 BVs for water pre-treated by coagulation. This shows potential for continuous precursor removal, particularly for the two coal-based media and the bone char GAC, provided 20-30% removal is acceptable. However, the relatively fast breakthrough to 50% DOC and tTHM/tHAA for the higher-DOC, substantially untreated water source (*Water A*) indicated limited capacity for long-term bulk removal of NOM for source waters having a high DBP-FP. Against this, GAC was found to be an effective polishing process for pre-clarified water (*Water B*), where longer term reduction in DOC and DBP precursors was recorded.

# 4 Conclusions

Granular activated carbon (GAC) media of various origins (coal, coconut shell and bovine bone), and providing a range of physical characteristics with reference to pore size, have been appraised with reference to their capacity for natural organic matter (NOM). Experiments comprised (a) batch adsorption experiments for determination of equilibrium capacity, and (b) tests on micro-columns to represent capacity under normal

436 operating conditions. Two different water sources were tested, a raw water with
437 rudimentary pretreatment (pressure sand filtration) and one pre-treated by full
438 clarification. The media capacity both for organic carbon and for chlorinated
439 disinfection byproduct formation propensity (DBPFP), with reference to both
440 trihalomethane (THM) and haloacetic acid (HAA) formation, was determined. The
441 applicability of $UV_{254}$ absorption as a surrogate for was also assessed.

442 Results revealed:

443 a. The 8 media tested were found to have a wide range of pore size distributions and
444 pore volume densities ($V_p$ in $cm^3/g$), specifically within the key range of 5-10 nm
445 ($V_{p,5\text{-}10}$).
446 b. There was no evidence of any selectivity for DBPFP removal by any of the media
447 tested: the ratio of THM and HAA concentrations generated from DOC in treated
448 waters did not change significantly between the different media.
449 c. In view of (b) above, $UV_{254}$ provided a reasonable surrogate measurement of both
450 DOC and DBPFP.
451 d. Batch adsorption tests provided a good indicator of media performance in terms of
452 NOM removal: ranking of media capacities from batch testing generated the same
453 sequence as that from microcolumn testing.
454 e. The media capacity, quantified in terms of bed volumes treated to breakthrough, was
455 found to correlate with the pore volume density of the 5-10 nm pores ($V_{p,5\text{-}10}$), in
456 terms of pore volume provided per unit mass of media. A 3-6 fold increase in
457 capacity was recorded for a change in $V_{p,5\text{-}10}$ from 0.005 to 0.042 $cm^3/g$.

f. Correlations were stronger for the water with rudimentary treatment than for the preclarified water due to both its increased organic carbon concentration and the hydrophobic content, the latter having a higher reactivity.

## Acknowledgments

The financial and practical support of EPSRC under the *STREAM* programme, EP/G037094/1, and Scottish Water are gratefully acknowledged.

## References

Ando, N., Matsui, Y., Kurotobi, R., Nakano, Y., Matsushita, T. and Ohno, K. (2010) 'Comparison of natural organic matter adsorption capacities of super-powdered activated carbon and powdered activated carbon.', Water Research, 44(14), 4127–36.

APHA (2012) Standard Methods for the Examination of Water and Wastewater. 22nd edn. Washington, DC: American Water Works Association, American Public Works Association, Water Environment Federation.

Aschermann, G., Zietzschmann, F., and Jekel, M. (2018), 'Influence of dissolved organic matter and activated carbon pore characteristics on organic micropollutant desorption', Water Research, 133, 123-131.

Bhatnagar, A. and Sillanpää, M. (2017) 'Removal of natural organic matter (NOM) and its constituents from water by adsorption - A review', Chemosphere, 166, 497–210.

Bougeard, C.M.M., Goslan, E.H., Jefferson, B. and Parsons, S.A. (2010) 'Comparison of the disinfection by-product formation potential of treated waters exposed to chlorine and monochloramine', Water Research, 44(3), 729–740.

Brunauer, S., Emmett, P.H. and Teller, E. (1938) 'Adsorption of Gases in Multimolecular Layers', Journal of the American Chemical Society, 60(2), 309–319.

Crittenden, J.C., Trussell, R.R., Hand, D.W., Howe, K.J., Tchobanoglous, G. and Borchardt, J.H. (2012) MWH Water Treatment Principles and Design. 3rd edn. New Jersey: Wiley.

Dastgheib, S. a, Karanfil, T. and Cheng, W. (2004) 'Tailoring activated carbons for enhanced removal of natural organic matter from natural waters', Carbon, 42(3), 547–557.

de Almeida Alves, A. A., de Oliveira Ruiz, G. L., Campos Martins. Nonato, T. C, Müller, L. C., Sens, M. L. (2019) Performance of the fixed-bed of granular activated carbon for the removal of pesticides from water supply, Environmental Technology,

490 40(15), 1977-1987.

491 de la Rubia, A., Rodríguez, M., León, V., and Prats, D. (2008), 'Removal of natural
492 organic matter and THM formation potential by ultra- and nanofiltration of surface
493 water', Water Research 42 (3) (2008) 714–722

494 Gibert, O., Lefèvre, B., Fernández, M., Bernat, X., Paraira, M. and Pons, M. (2013)
495 'Fractionation and removal of dissolved organic carbon in a full-scale granular activated
496 carbon filter used for drinking water production.', Water Research, 47(8), 2821–9.

497 Golea, D.M., Upton, A., Jarvis, P., Moore, G., Sutherland, S.T., Parsons, S.A. and Judd,
498 S.J. (2017) 'THM and HAA formation from NOM in raw and treated surface waters',
499 Water Research, 112, 226–235.

500 Goslan, E.H., Krasner, S.W., Bower, M., Rocks, S.A., Holmes, P., Levy, L.S. and
501 Parsons, S.A. (2009) 'A comparison of disinfection by-products found in chlorinated
502 and chloraminated drinking waters in Scotland', Water Research, 43(18), 4698–4706.

503 Graf, K.C., Cornwell, D.A. and Boyer, T.H. (2014) 'Removal of dissolved organic
504 carbon from surface water by anion exchange and adsorption: Bench-scale testing to
505 simulate a two-stage countercurrent process', Separation and Purification Technology,
506 122, 523–532.

507 Greiner, B.G., Shimabuku, K.K. and Summers, R.S. (2018) 'Influence of biochar
508 thermal regeneration on sulfamethoxazole and dissolved organic matter adsorption',
509 Environmental Science Water Research & Technology, 4 Royal Society of Chemistry,
510 169–174.

511 Gui, H. J., Li, F. S., Wei, Y. F., and Yamada, T. (2018) 'Adsorption characteristics of
512 natural organic matter on activated carbons with different pore size distribution',
513 International Journal of Environmental Science and Technology, 15(8), 1619-1628.

514 Hoslett, J., Massara, T.M., Malamis, S., Ahmad, D., van den Boogaert, I., Katsou, E.,
515 Ahmad, B., Ghazal, H., Simons, S., Wrobel, L. and Jouhara, H. (2018) 'Surface water fi
516 ltration using granular media and membranes : A review', Science of the Total
517 Environment, 639, 1268–1282.

518 Iriarte-Velasco, U., Álvarez-Uriarte, J. I., Chimeno-Alaníc, N., and González-Velasco,
519 J. R. (2008), 'Natural organic matter adsorption onto granular activated carbons:
520 Implications in the molecular weight and disinfection byproducts formation', Industrial
521 and Engineering Chemistry Research, 47(20), 7868-7876.

522 Karanfil, T., Kitis, M., Kilduff, J.E. and Wington, A. (1999) 'Role of Granular
523 Activated Carbon Surface Chemistry on the Adsorption of Organic Compounds . 2 .
524 Natural Organic Matter', Environmental Science and Technology, 33(18), 3225–3233.

525 Karapinar, N., Uyak, V., Soylu, S. and Topal, T. (2014) 'Seasonal Variations of NOM
526 Composition and their Reactivity in a Low Humic Water', Environmental Progress &
527 Sustainable Energy, 33(3), 962–971.

528 Lastoskie, C., Gubbins, K. E., and Quirke, N. (1993) 'Pore size distribution analysis of
529 microporous carbons: A density functional theory approach', Journal of Physical

Chemistry, 97(18), 4786-4796.

Li, F., Yuasa, A., Katamine, Y. and Tanaka, H. (2007) 'Breakthrough of natural organic matter from fixed bed adsorbers: investigations based on size-exclusion HPLC', Adsorption, 13(5–6), 569–577.

Liao, X. B., Cheng, Y. S., Liu, Z. H., Shen, L. L., Zhao, L., Chen, C., Li, F. and Zhang, X. J. (2019) 'Performance of BAC for DBPs precursors' removal for one year with micro-polluted lake water in East-China', Environmental Technology.

Matilainen, A., Vieno, N. and Tuhkanen, T. (2006) 'Efficiency of the activated carbon filtration in the natural organic matter removal', Environment International, 32(3), 324–31.

Moore, B.C., Cannon, F.S., Westrick, J. a., Metz, D.H., Shrive, C. a., DeMarco, J. and Hartman, D.J. (2001) 'Changes in GAC pore structure during full-scale water treatment at Cincinnati: a comparison between virgin and thermally reactivated GAC', Carbon, 39(6), 789–807.

Moreno, J.C., Gómez, R. and Giraldo, L. (2010) 'Removal of Mn, Fe, Ni and Cu Ions from Wastewater Using Cow Bone Charcoal', Materials, 3, 452–466.

Ndiweni, S. N., Chys, M., Chaukura, N., Van Hulle, S. W. H. and Nkambule, T. T. I. (2019) 'Assessing the impact of environmental activities on natural organic matter in South Africa and Belgium', Environmental Technology, 40 (13), 1756-1768.

Nili-Ahmadabadi, A.R.M.R.G.G.A. (2011) 'Adsorption of Escherichia coli Using Bone Char', Journal of Applied Science and Environment Management, 15(1), 57–62.

Philippe, K. K., Hans, C., MacAdam, J., Jefferson, B., Hart, J. and Parsons, S. A (2010). Photocatalytic oxidation, GAC and biotreatment combinations: an alternative to the coagulation of hydrophilic rich waters?' Environmental Technology, 31(13), pp. 1423–34.

Piai, L., Dykstra, J. E., Adishakti, M. G., Blokland, M., Langenhoff, A. A. M., & van der Wal, A. (2019). Diffusion of hydrophilic organic micropollutants in granular activated carbon with different pore sizes. Water Research, 162, 518-527.

Ratnayaka, D.D., Brandt, M.J. and Johnson, K.M. (2008) TWORT's Water Supply. 6th edn. .

Reckhow, D.A. and Singer, P.C. (2010) 'Formation and Control of Disinfection By-Products', in Edzwald, J. K. (ed.) Water Quality & Treatment : A Handbook on Drinking Water: A Handbook on Drinking Water. 6th edn. New York: McGraw-Hill Publishing, 1–60.

Shimabuku, K. K., Paige, J. M., Luna-Aguero, M., & Summers, R. S. (2017). Simplified modeling of organic contaminant adsorption by activated carbon and biochar in the presence of dissolved organic matter and other competing adsorbates. Environmental Science and Technology, 51(17), 10031-10040.

Summers, R.S., Hooper, S. M., Solarik, G., Owen, D. M., Hong, S. (1995) 'Bench-Scale Evaluation of GAC for NOM Control', Journal American Water Works Association,

570 87(8), 69–80.

571 Summers, R.S., Ph, D., Knappe, D.R.U., Carolina, N. and States, U. (2010) 'Adsorption
572 of Organic Compounds by Activated Carbon', in Edzwald, J. K. (ed.) Water Quality &
573 Treatment : A Handbook on Drinking Water: A Handbook on Drinking Water. 6th edn.
574 New York: McGraw-Hill Publishing, 1–106.

575 Sun, Y., Angelotti, B., Brooks, M., Dowbiggin, B., Evans, P.J., Devins, B. and Wang,
576 Z. (2018) 'A pilot-scale investigation of disinfection by-product precursors and trace
577 organic removal mechanisms in ozone-biologically activated carbon treatment for
578 potable reuse', Chemosphere, 210, 539–549.

579 USEPA (1998) 'National Primary Drinking Water Regulations: Disinfectants and
580 Disinfection Byproducts. U.S. Environmental Protection Agency', Federal Register,
581 63(241), 69390–69476.

582 USEPA (2010) Stage 2 disinfectants and disinfection byproducts rule. Consecutive
583 Systems Guidance Manual EPA 815-R-09-017.

584 Valdivia-Garcia, M., Weir, P., Frogbrook, Z., Graham, D.W. and Werner, D. (2016)
585 'Climatic, Geographic and Operational Determinants of Trihalomethanes (THMs) in
586 Drinking Water Systems', Scientific Reports, 6, 35027.

587 Velten, S., Knappe, D.R.U., Traber, J., Kaiser, H.-P., von Gunten, U., Boller, M. and
588 Meylan, S. (2011) 'Characterization of natural organic matter adsorption in granular
589 activated carbon adsorbers', Water Research, 45(13), 3951–9.

590 Zeng, J., Chen, S., Wan, K., Li, J., Hu, D., Zhang, S. and Yu, X. (2019) 'Study of
591 biological up-flow roughing filters designed for drinking water pretreatment in rural
592 areas: using ceramic media as filter material', Environmental Technology, *in press*.

593

Figure 1

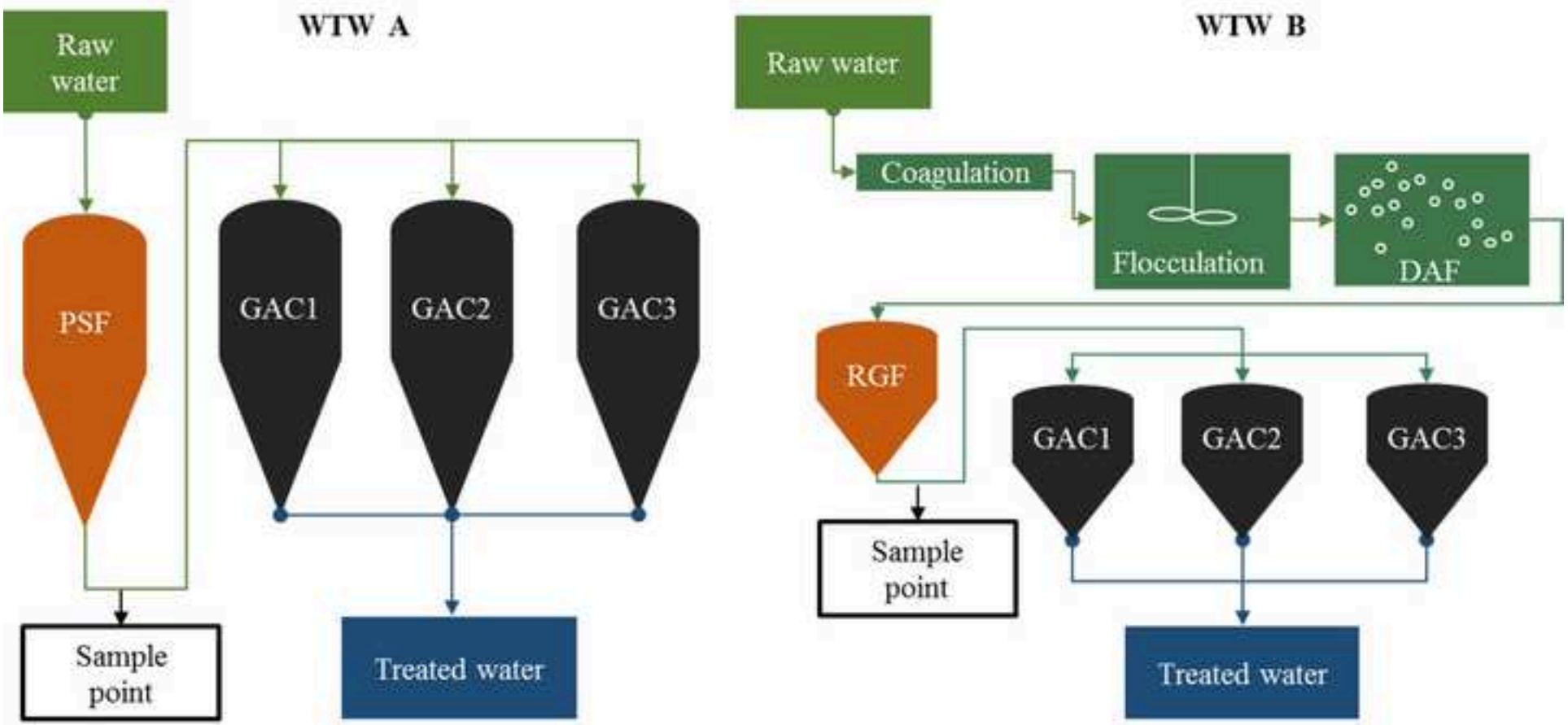
WTW A
Raw water
PSF
GAC1
GAC2
GAC3
Sample point
Treated water
WTW B
Raw water
Coagulation
Flocculation
DAF
RGF
GAC1
GAC2
GAC3
Sample point
Treated water

Figure 2a

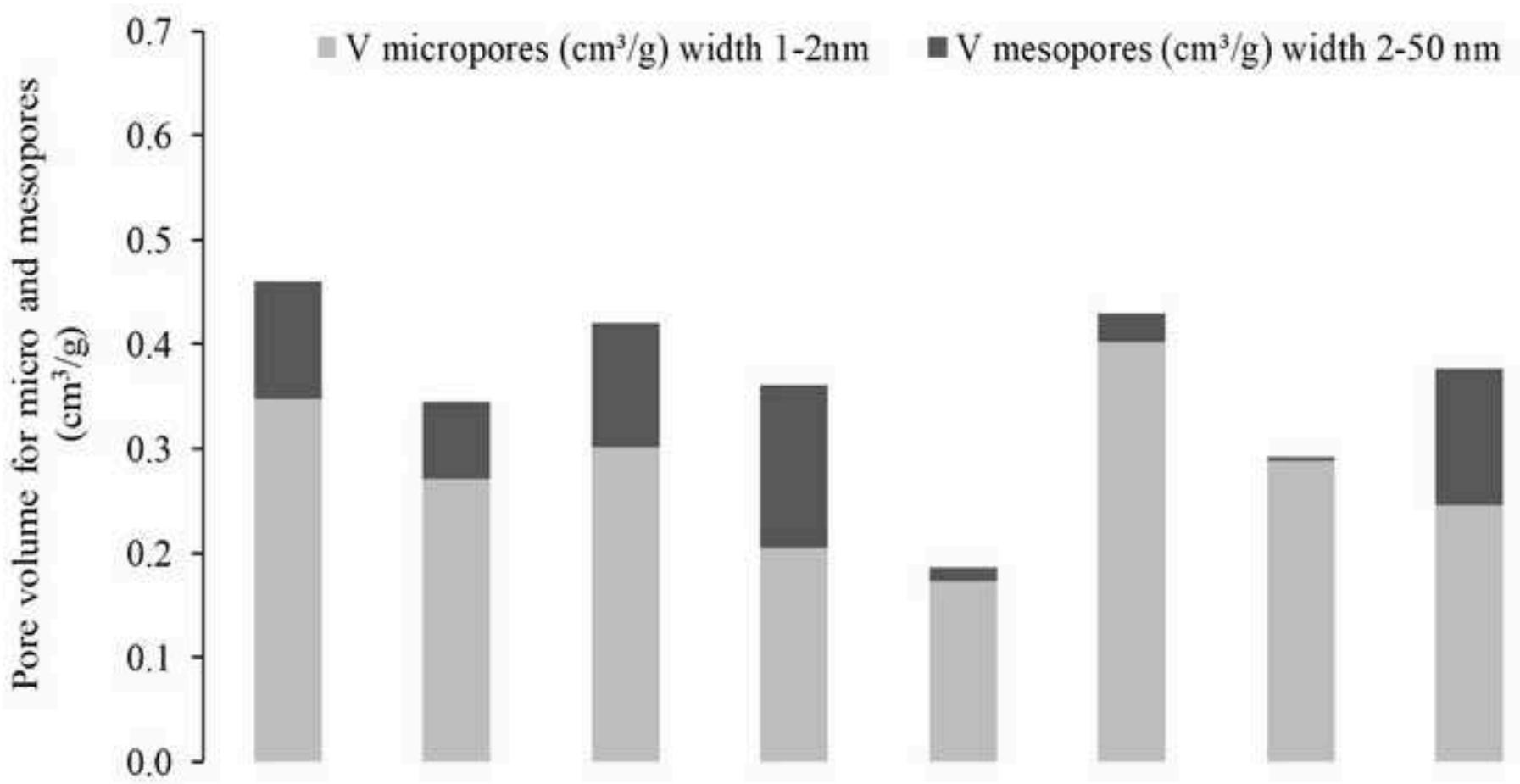
V micropores (cm³/g) width 1-2nm
V mesopores (cm³/g) width 2-50 nm
Pore volume for micro and mesopores (cm³/g)
0.7
0.6
0.5
0.4
0.3
0.2
0.1
0.0

Figure 2b

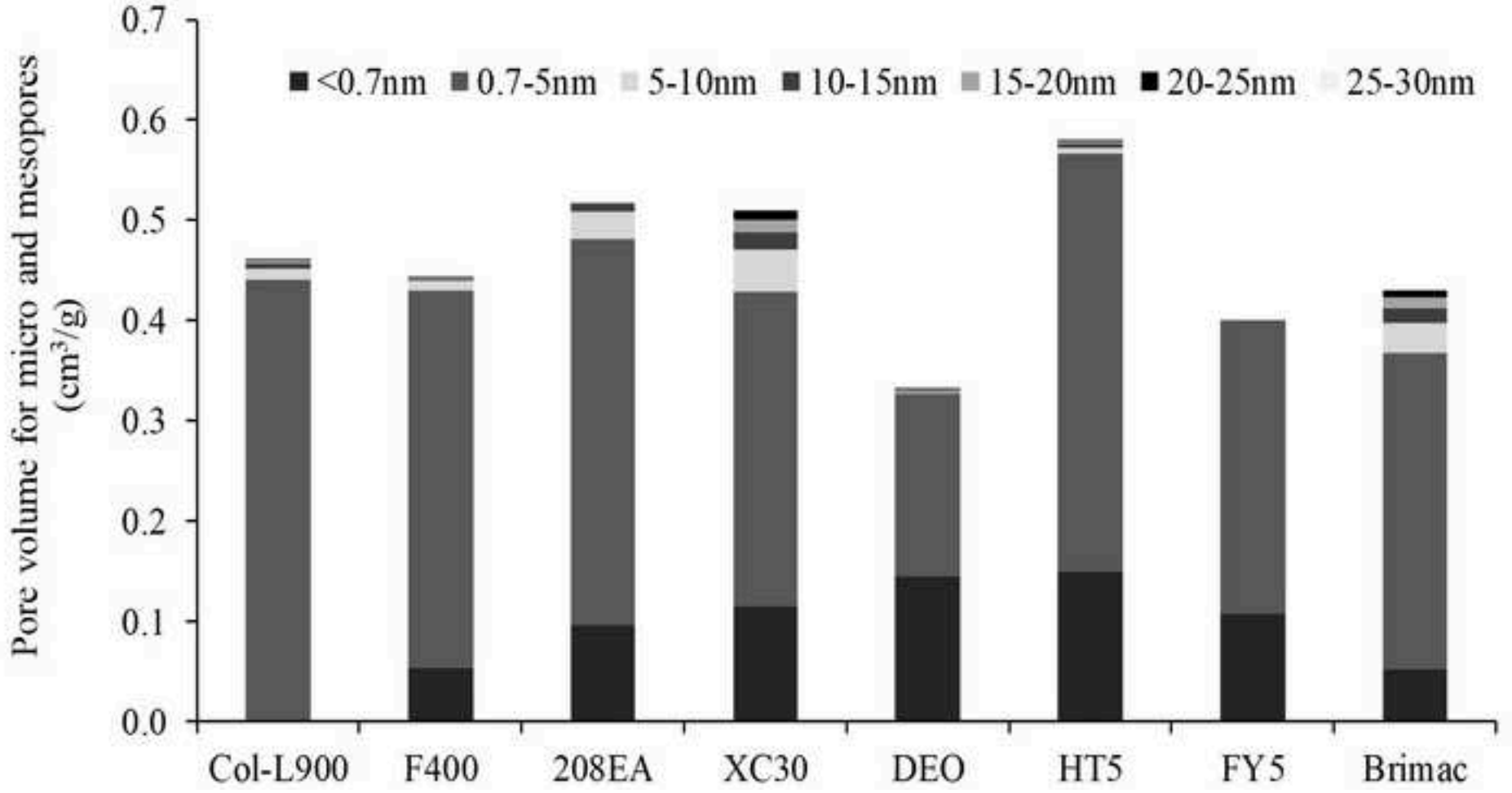
Pore volume for micro and mesopores (cm³/g)
0.7
0.6
0.5
0.4
0.3
0.2
0.1
0.0
<0.7nm
0.7-5nm
5-10nm
10-15nm
15-20nm
20-25nm
25-30nm
Col-L900
F400
208EA
XC30
DEO
HT5
FY5
Brimac

Figure 3

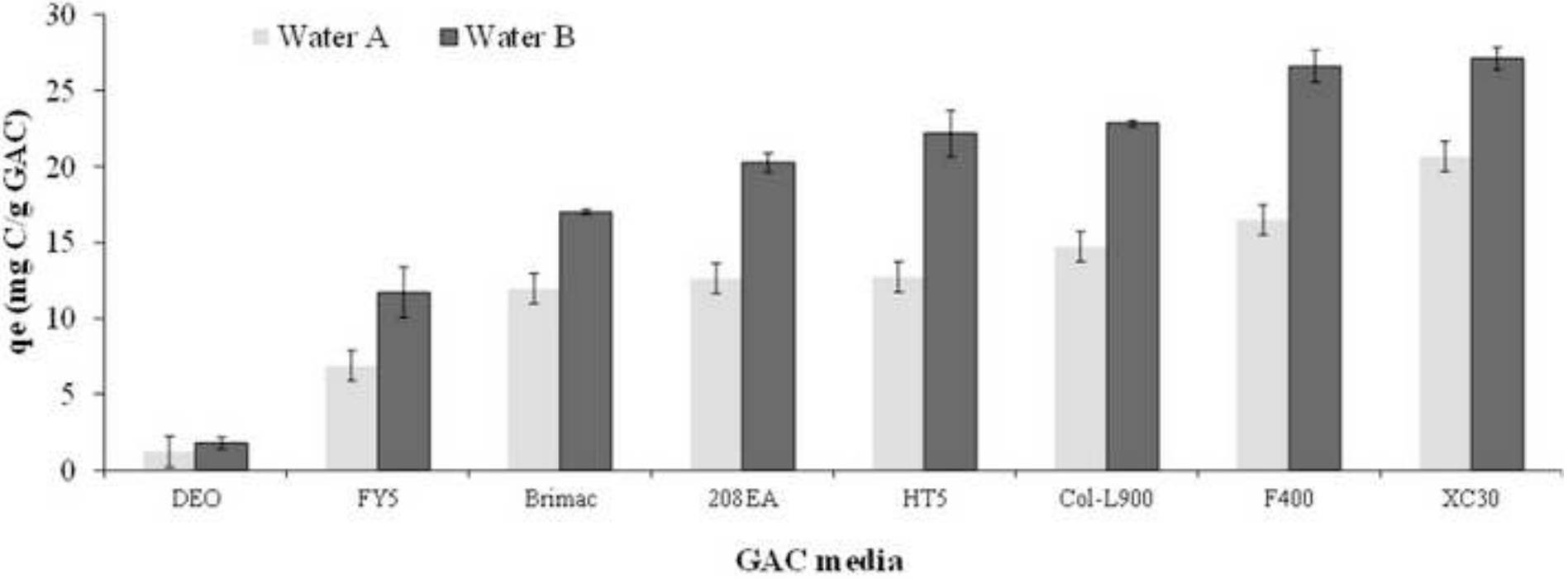
Water A
Water B
qe (mg C/g GAC)
30
25
20
15
10
5
0
DEO
FY5
Brimac
208EA
HT5
Col-L900
F400
XC30
GAC media

Figure 4a

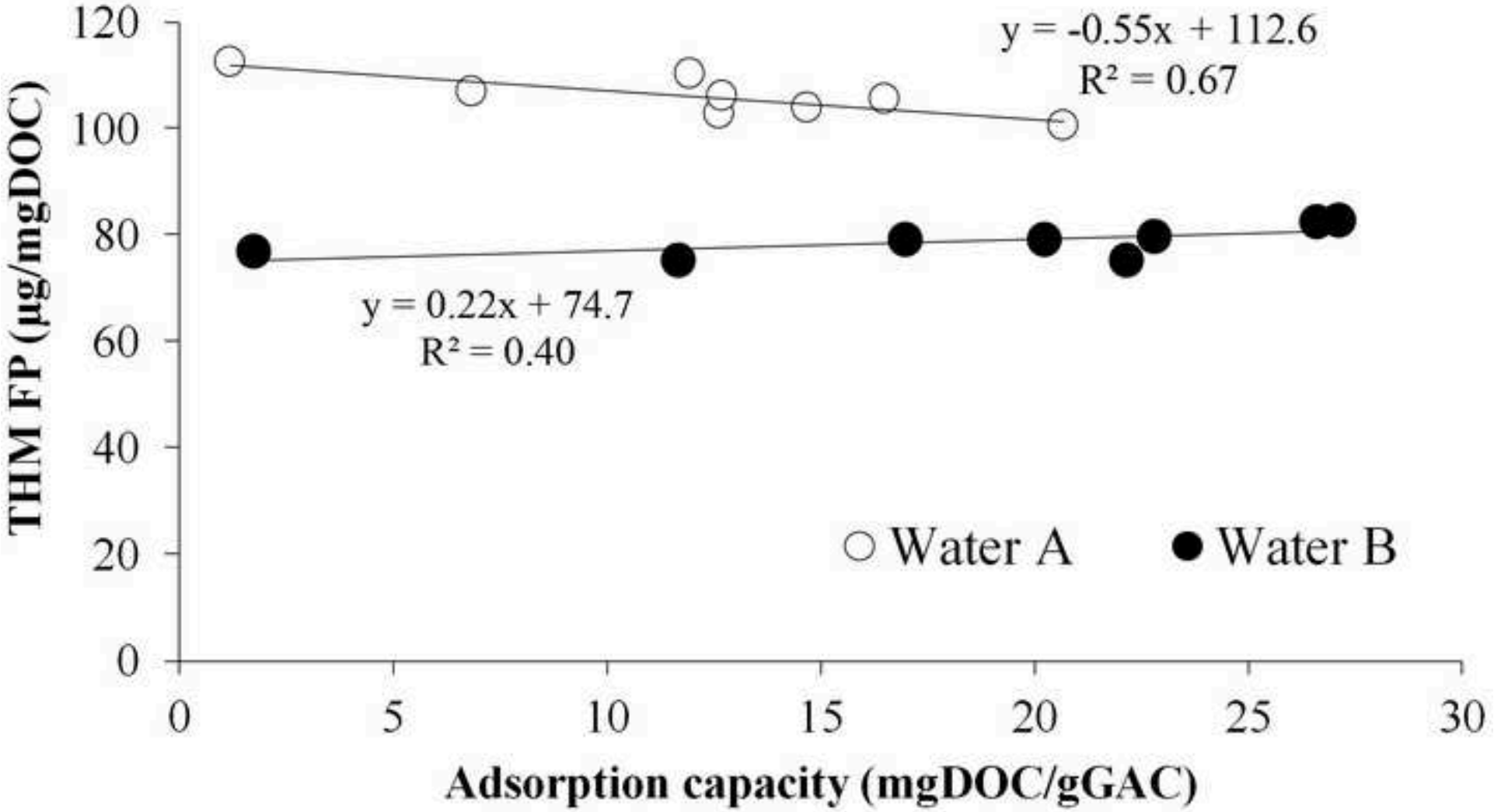
y = -0.55x + 112.6
R² = 0.67
y = 0.22x + 74.7
R² = 0.40
Water A
Water B
THM FP (µg/mgDOC)
Adsorption capacity (mgDOC/gGAC)
0
20
40
60
80
100
120
0
5
10
15
20
25
30

Figure 4b

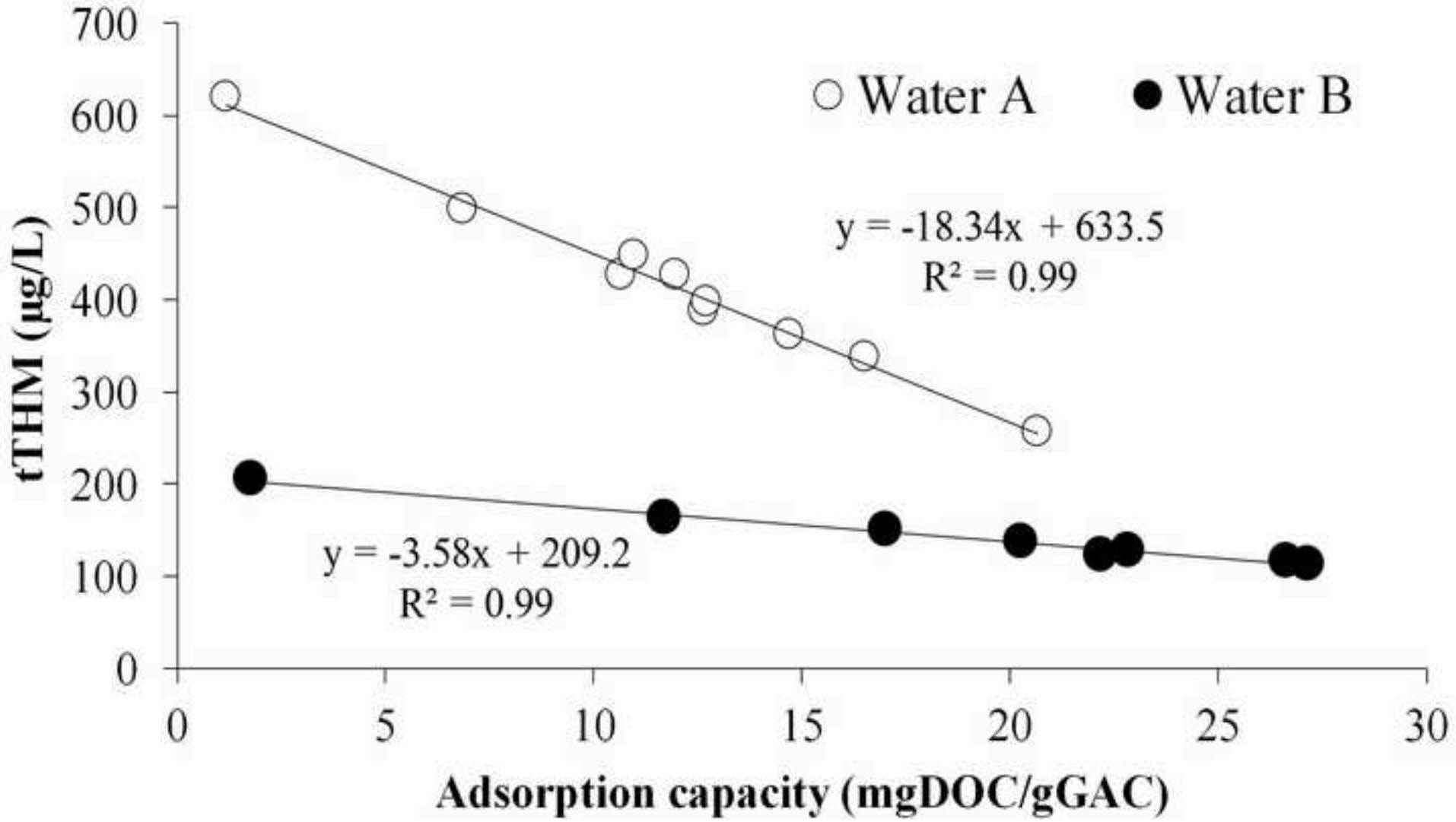
700
600
500
400
300
200
100
0
tTHM (µg/L)
Water A
Water B
y = -18.34x + 633.5
R² = 0.99
y = -3.58x + 209.2
R² = 0.99
0
5
10
15
20
25
30
Adsorption capacity (mgDOC/gGAC)

Figure 5a

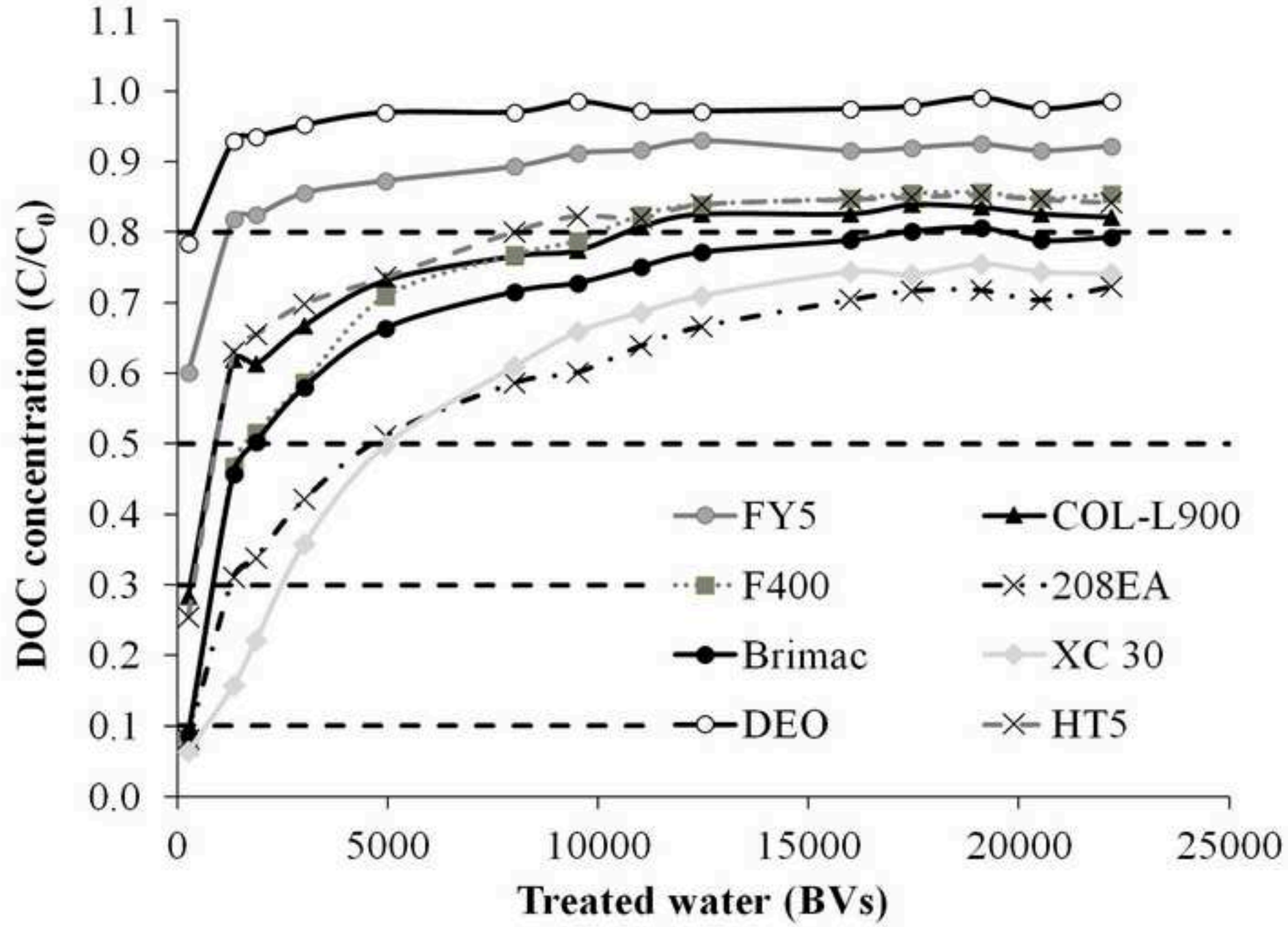
DOC concentration (C/C0)
1.1
1.0
0.9
0.8
0.7
0.6
0.5
0.4
0.3
0.2
0.1
0.0
0
5000
10000
15000
20000
25000
Treated water (BVs)
FY5
COL-L900
F400
208EA
Brimac
XC 30
DEO
HT5

Figure 5b

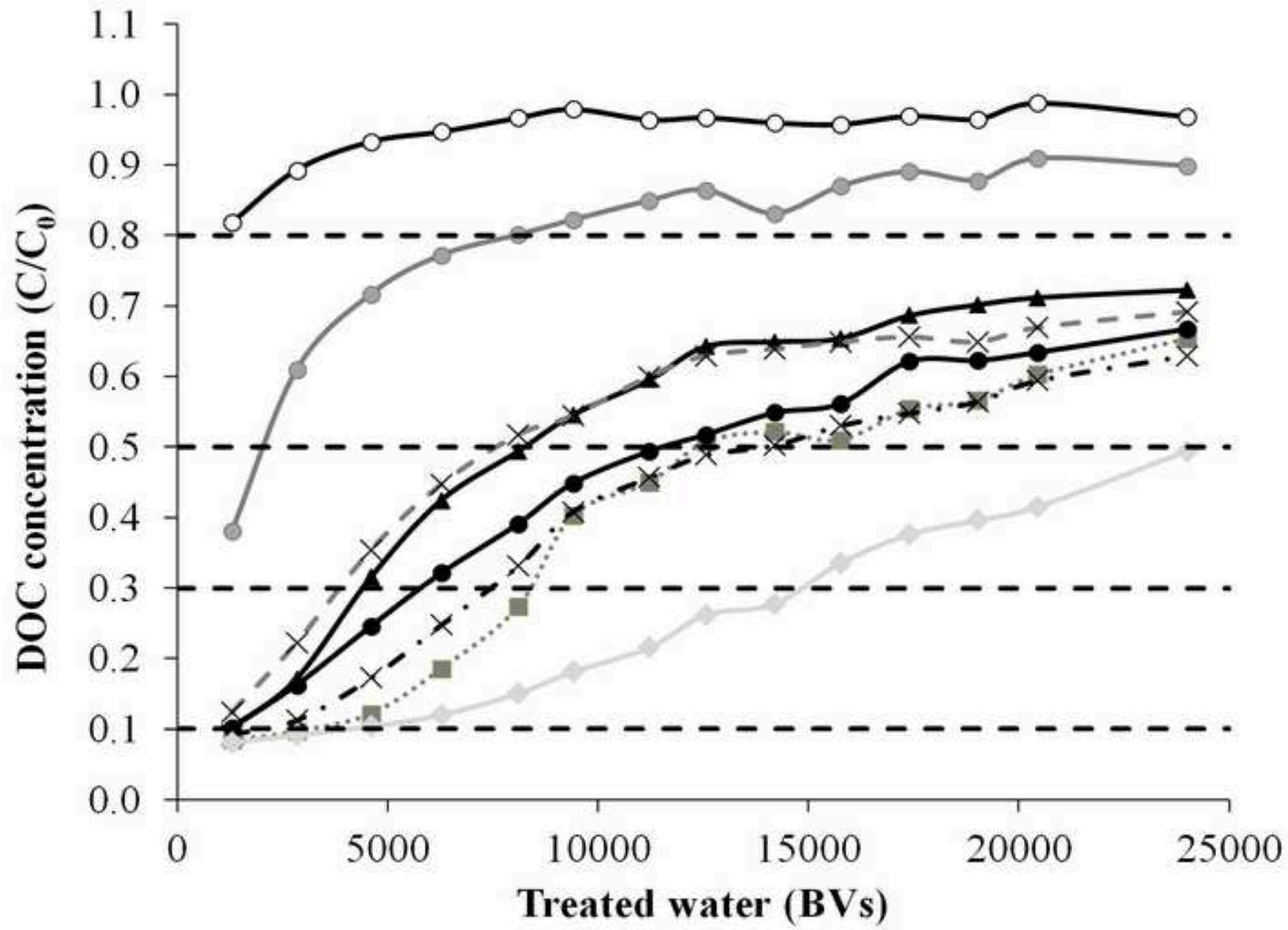
1.1
1.0
0.9
0.8
0.7
0.6
0.5
0.4
0.3
0.2
0.1
0.0
DOC concentration (C/C0)
0
5000
10000
15000
20000
25000
Treated water (BVs)

Figure 5c

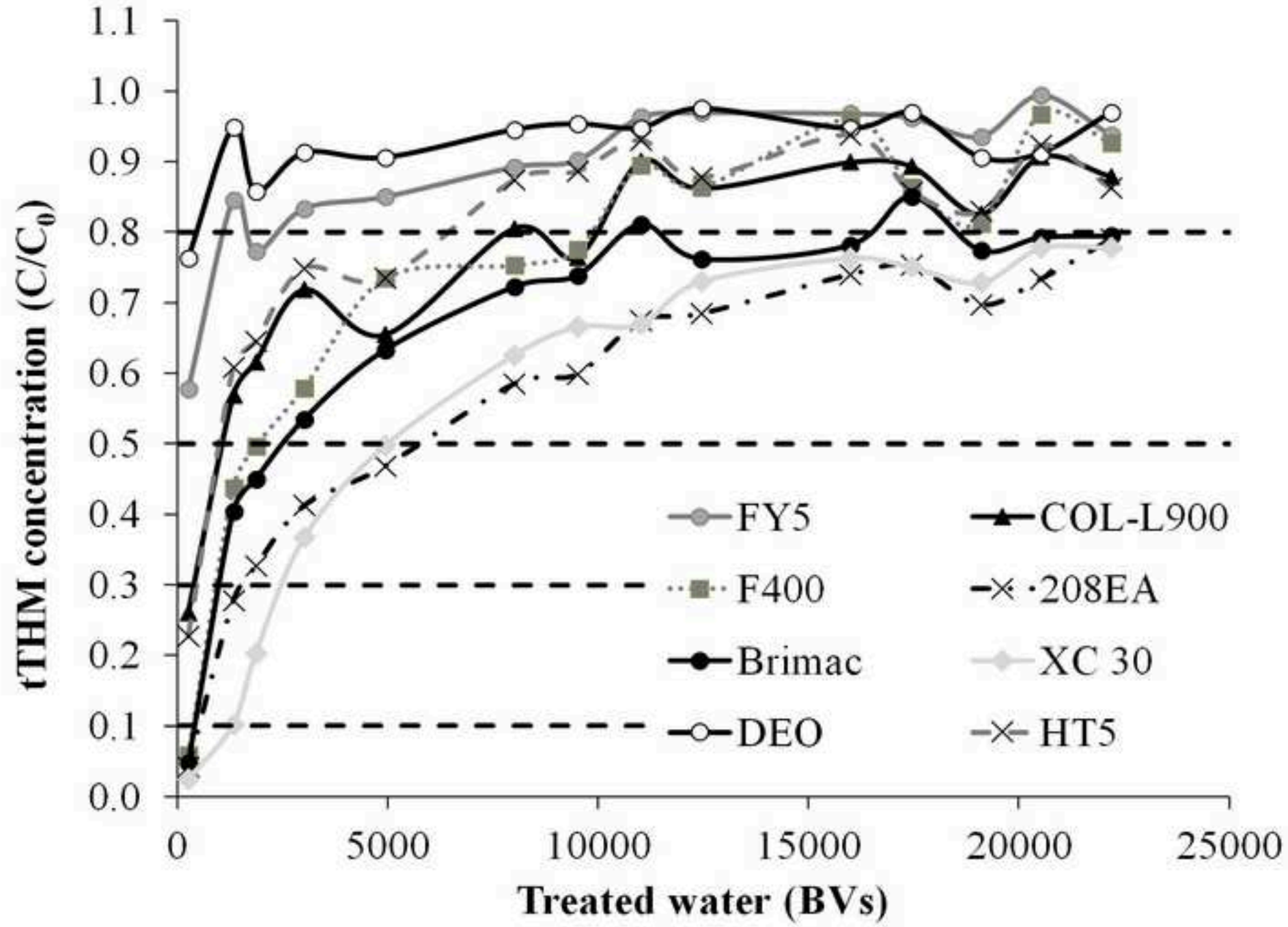
1.1
1.0
0.9
0.8
0.7
0.6
0.5
0.4
0.3
0.2
0.1
0.0
tTHM concentration (C/C0)
0
5000
10000
15000
20000
25000
Treated water (BVs)
FY5
COL-L900
F400
208EA
Brimac
XC 30
DEO
HT5

Figure 5d

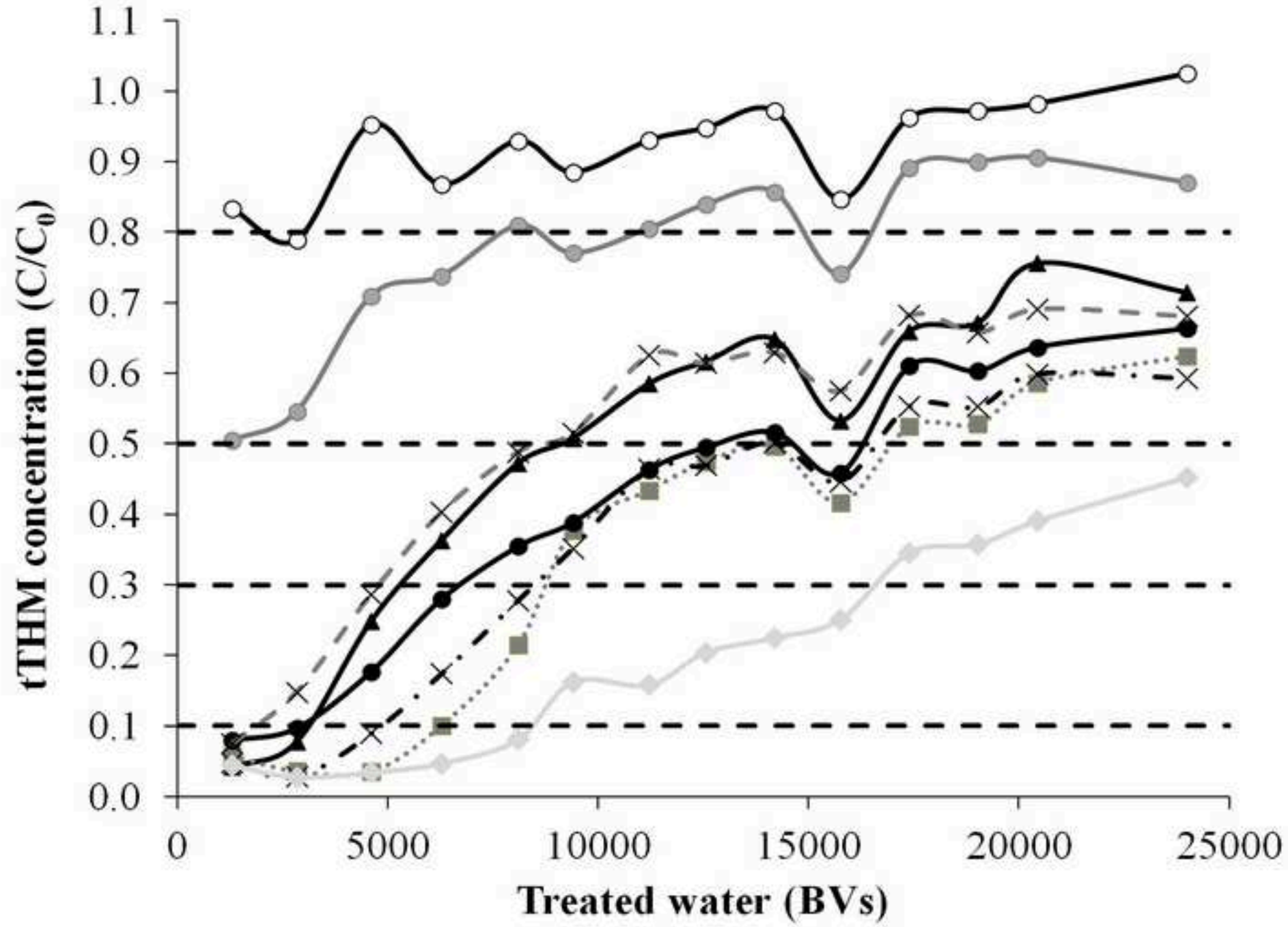
tTHM concentration (C/C0)
1.1
1.0
0.9
0.8
0.7
0.6
0.5
0.4
0.3
0.2
0.1
0.0
0
5000
10000
15000
20000
25000
Treated water (BVs)

Figure 5e

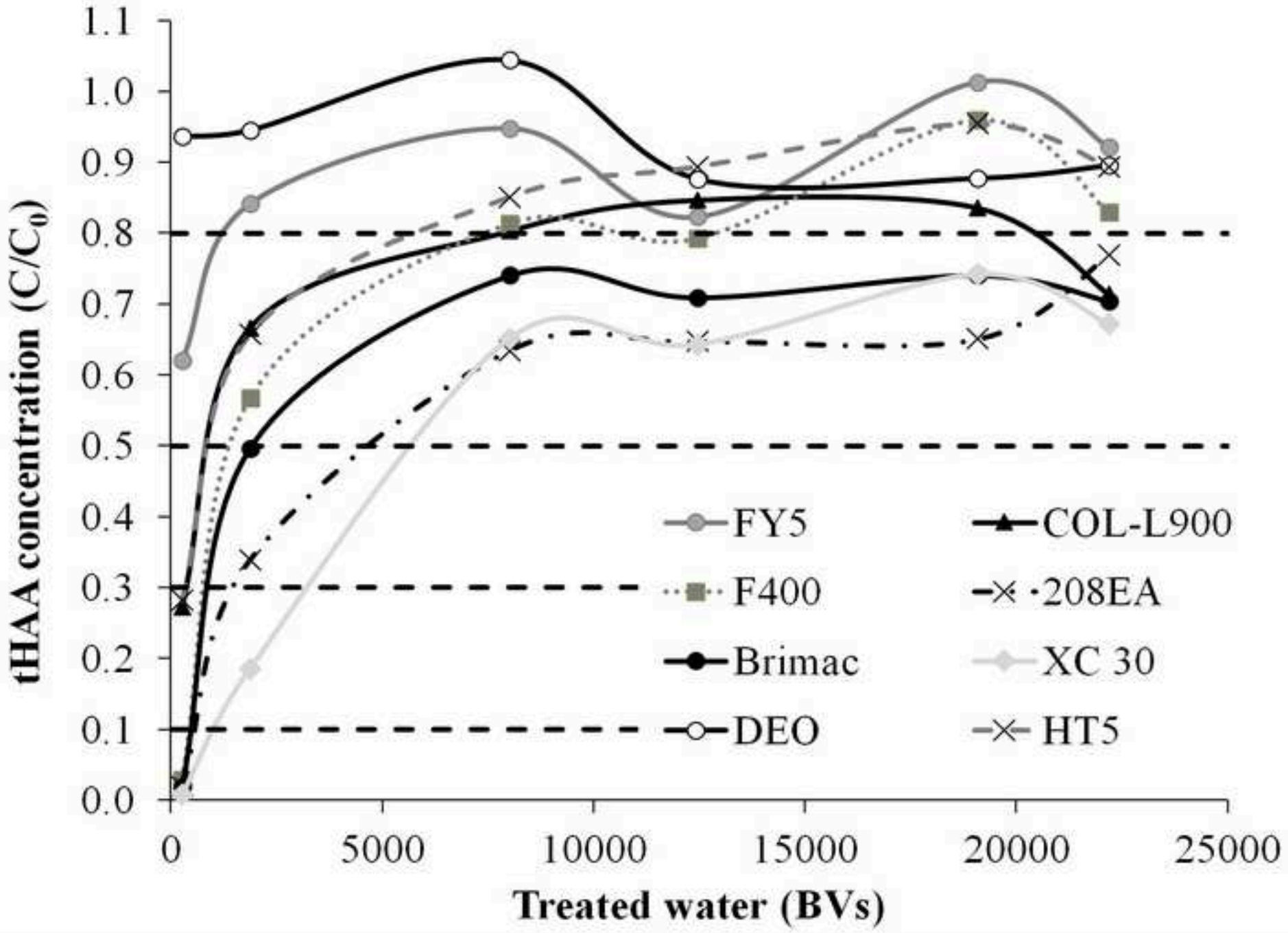
1.1
1.0
0.9
0.8
0.7
0.6
0.5
0.4
0.3
0.2
0.1
0.0
tHAA concentration (C/C0)
0
5000
10000
15000
20000
25000
Treated water (BVs)
FY5
COL-L900
F400
208EA
Brimac
XC 30
DEO
HT5

Figure 5f

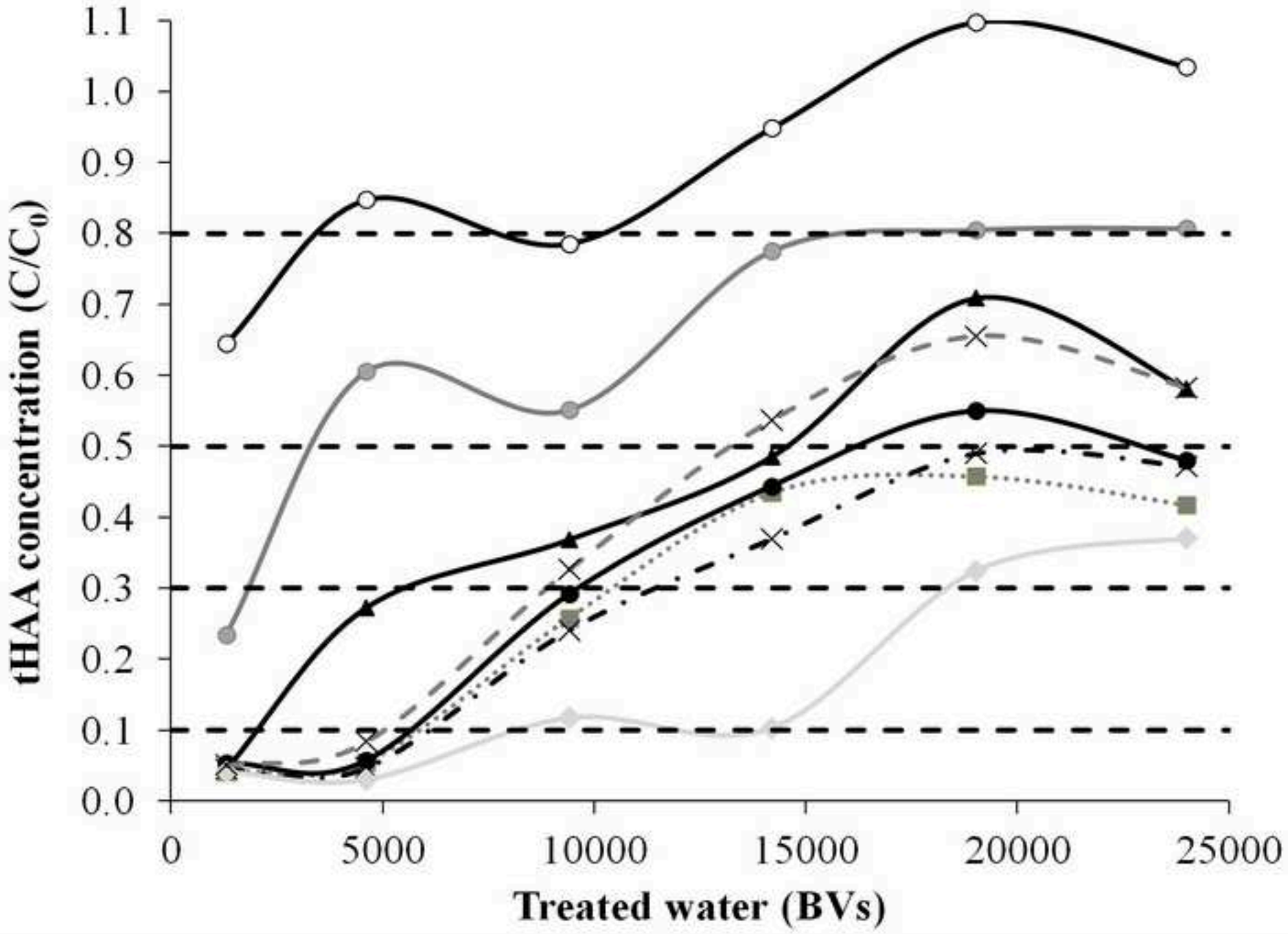
1.1
1.0
0.9
0.8
0.7
0.6
0.5
0.4
0.3
0.2
0.1
0.0
tHAA concentration (C/C0)
0
5000
10000
15000
20000
25000
Treated water (BVs)

Figure 6a

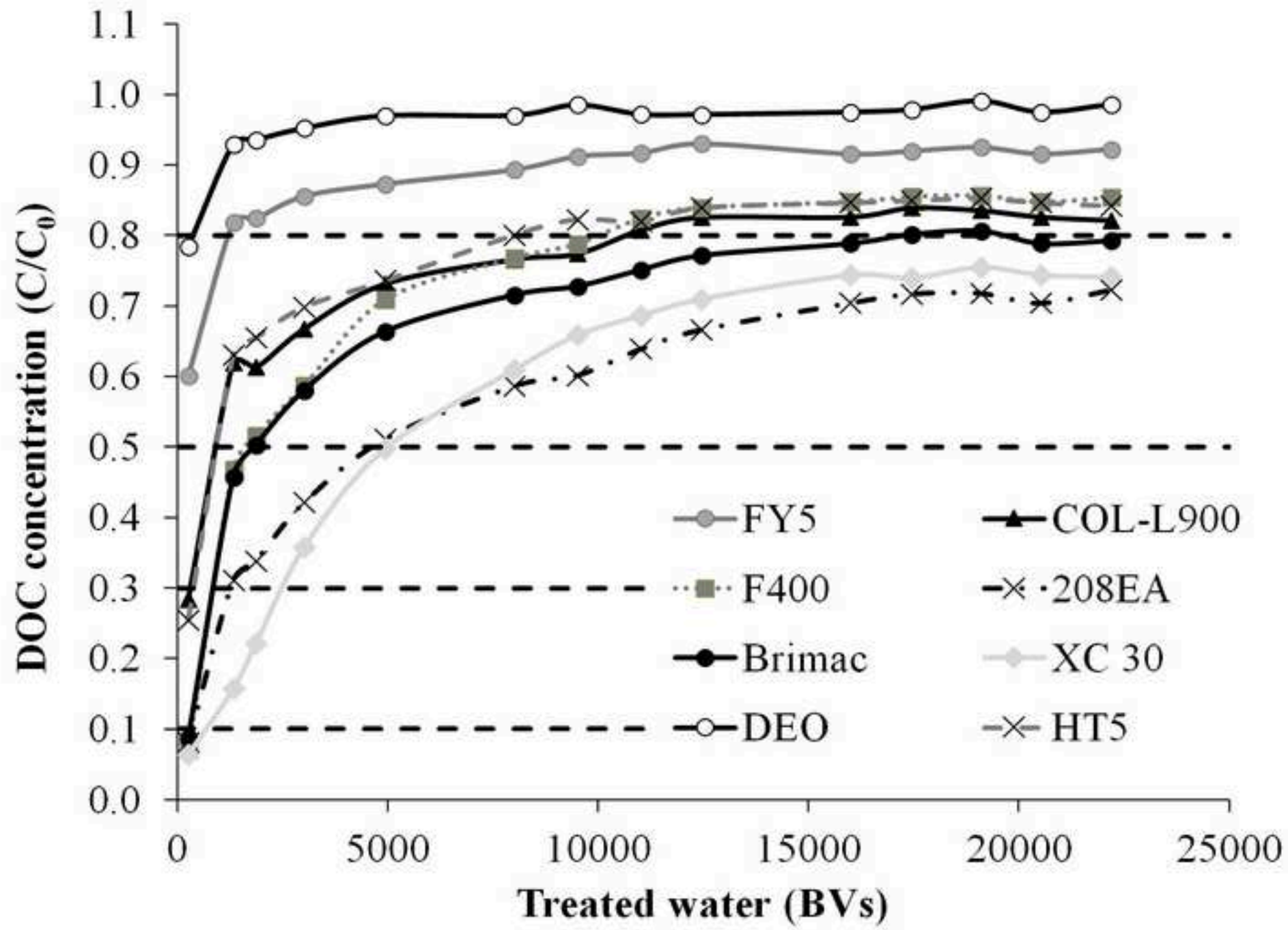
DOC concentration (C/C0)
1.1
1.0
0.9
0.8
0.7
0.6
0.5
0.4
0.3
0.2
0.1
0.0
0
5000
10000
15000
20000
25000
Treated water (BVs)
FY5
COL-L900
F400
208EA
Brimac
XC 30
DEO
HT5

Figure 6b

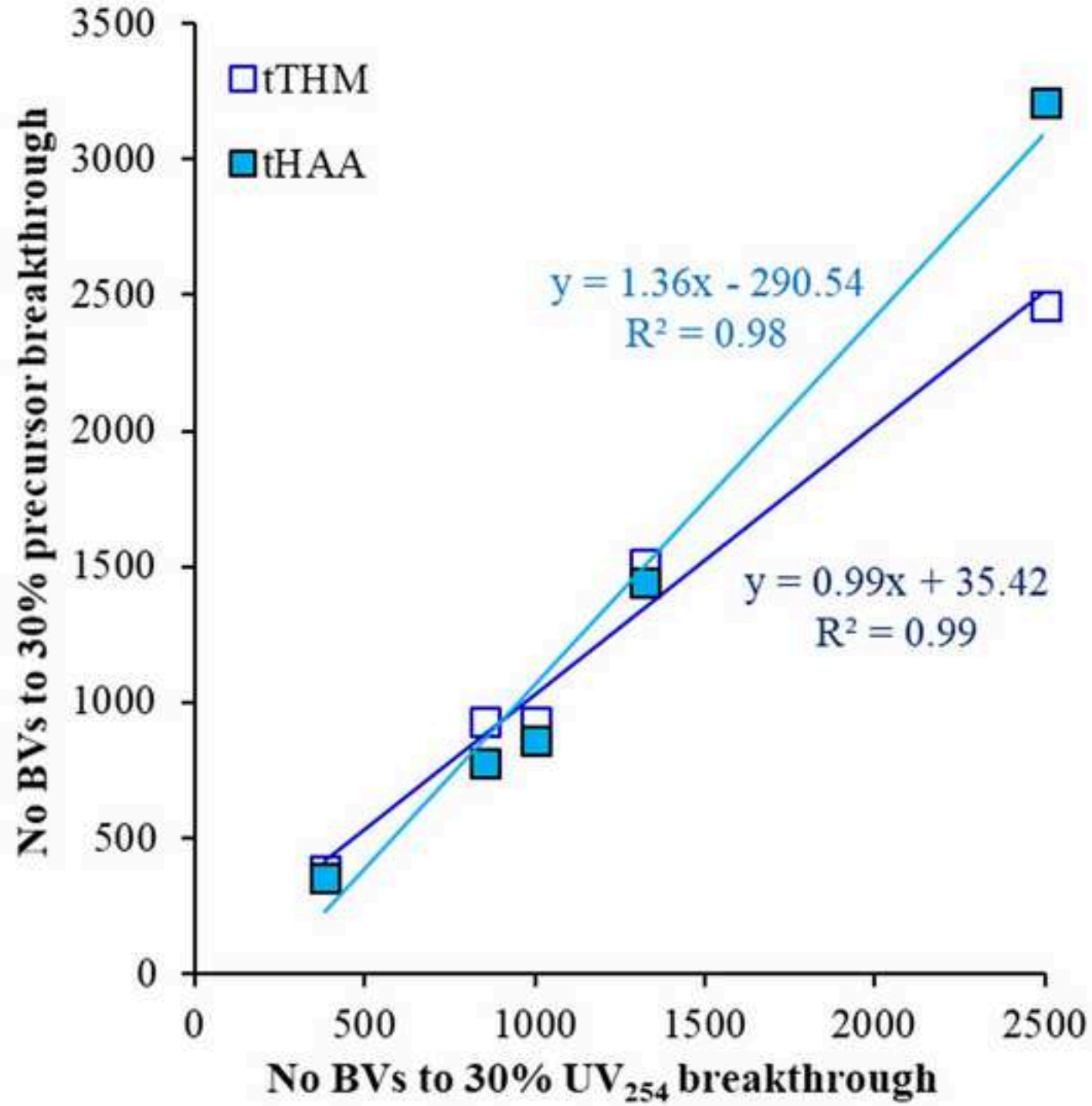
tTHM
tHAA
y = 1.36x - 290.54
R² = 0.98
y = 0.99x + 35.42
R² = 0.99
No BVs to 30% precursor breakthrough
No BVs to 30% UV254 breakthrough
0
500
1000
1500
2000
2500
3000
3500

Figure 6c

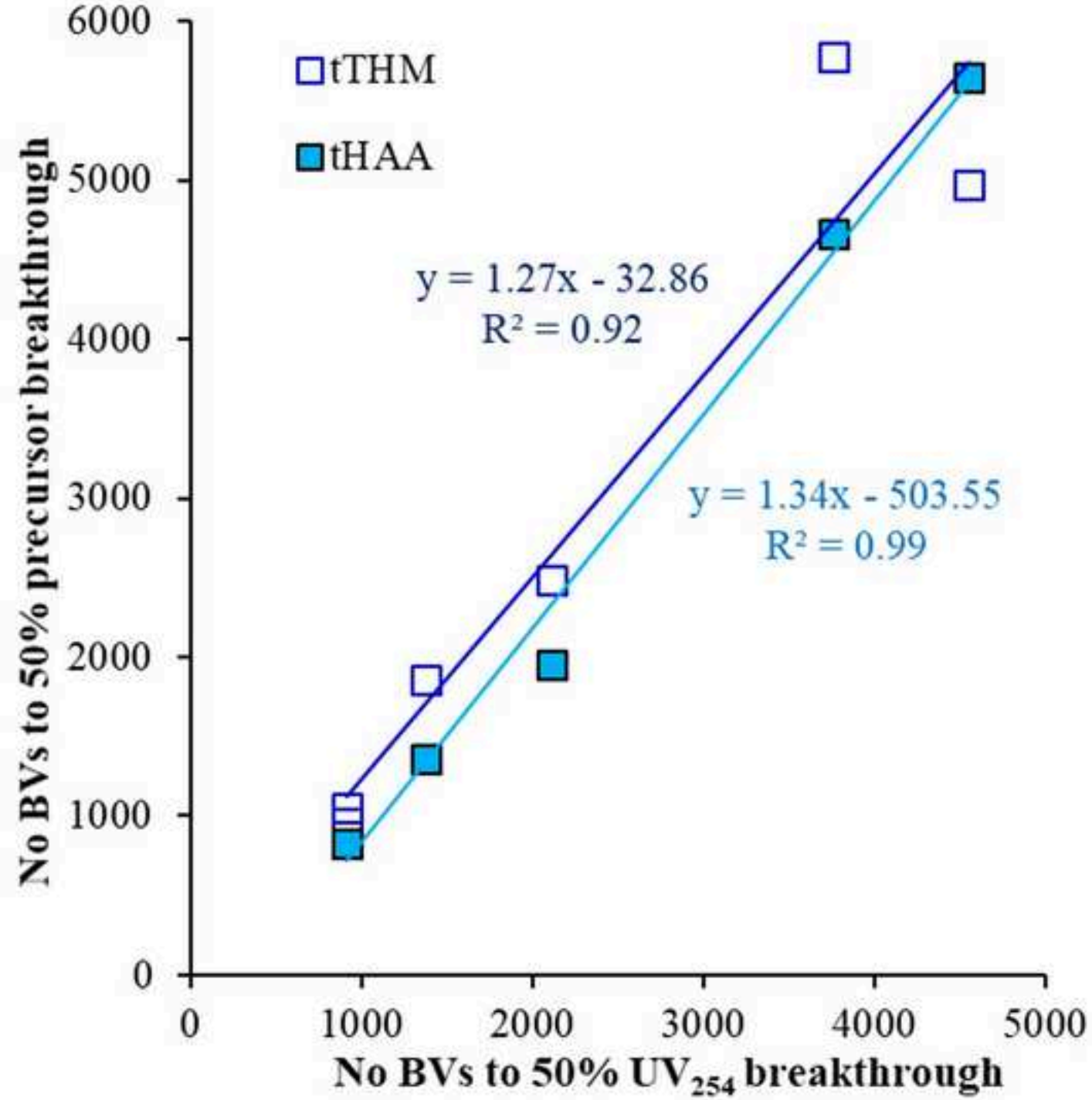
6000
5000
4000
3000
2000
1000
0
tTHM
tHAA
y = 1.27x - 32.86
R² = 0.92
y = 1.34x - 503.55
R² = 0.99
No BVs to 50% precursor breakthrough
0
1000
2000
3000
4000
5000
No BVs to 50% UV254 breakthrough

Figure 6d

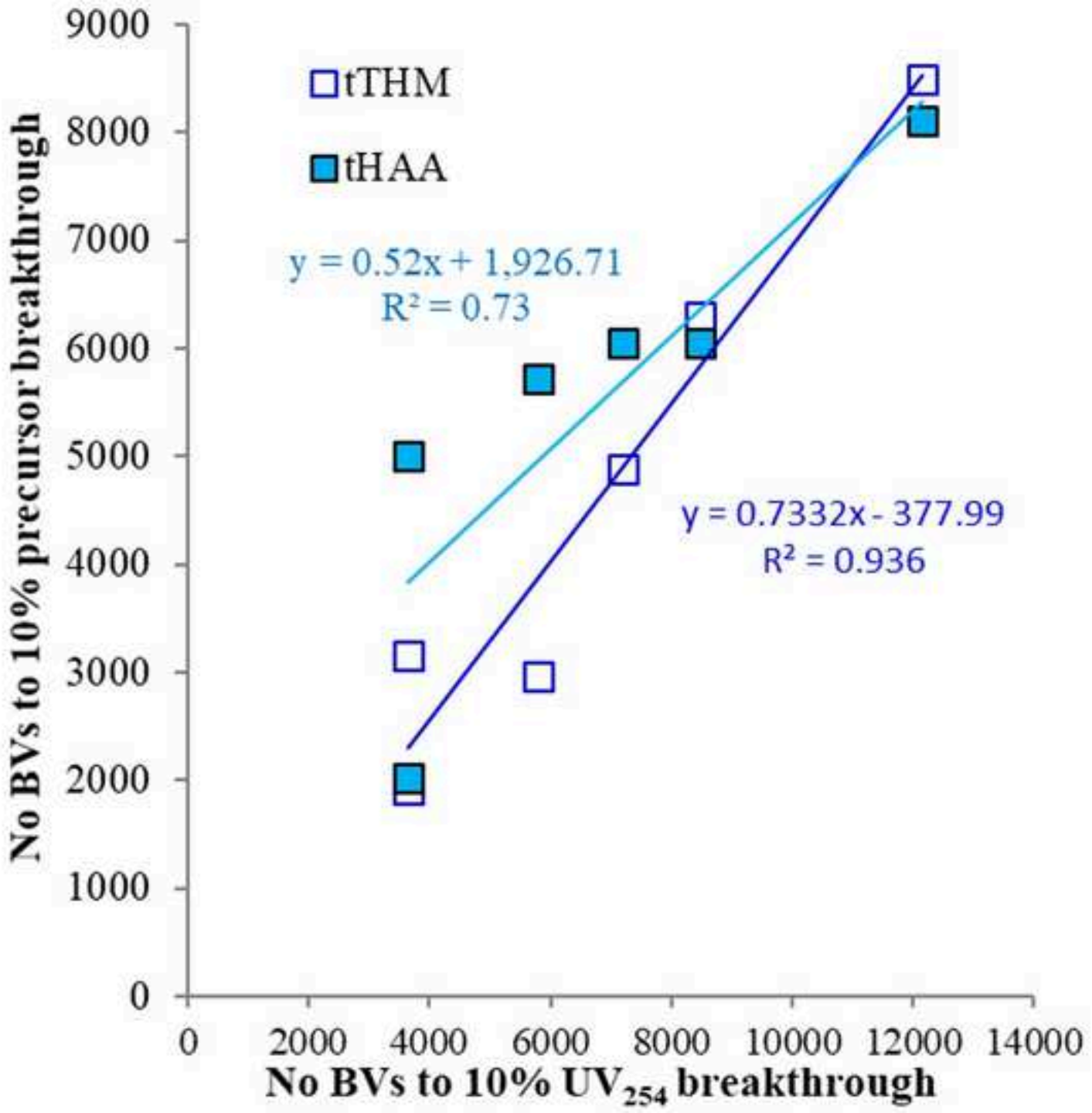
9000
8000
7000
6000
5000
4000
3000
2000
1000
0
No BVs to 10% precursor breakthrough
tTHM
tHAA
y = 0.52x + 1,926.71
R² = 0.73
y = 0.7332x - 377.99
R² = 0.936
0
2000
4000
6000
8000
10000
12000
14000
No BVs to 10% UV254 breakthrough

Figure 6e

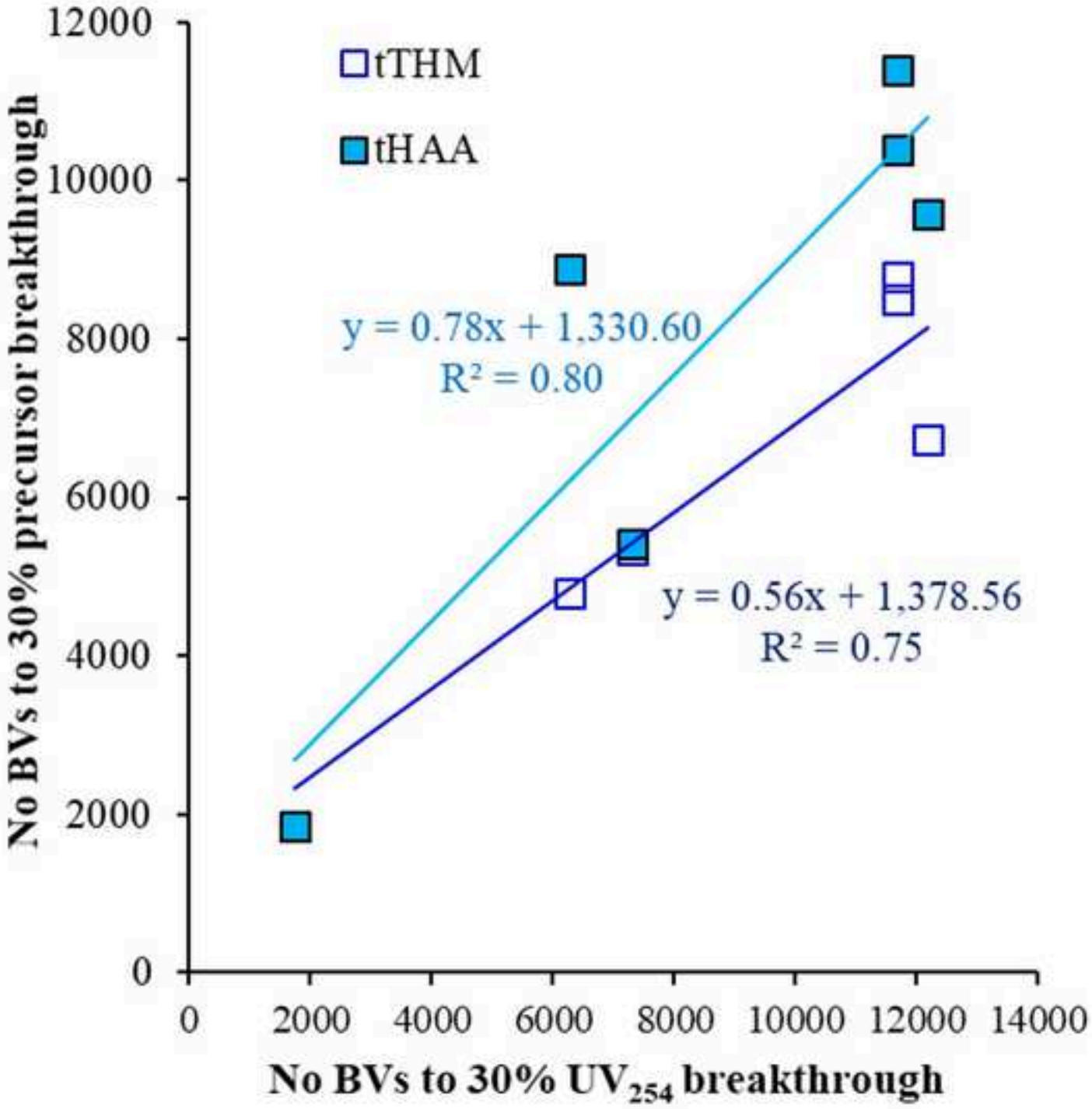
12000
10000
8000
6000
4000
2000
0
tTHM
tHAA
y = 0.78x + 1,330.60
R² = 0.80
y = 0.56x + 1,378.56
R² = 0.75
No BVs to 30% precursor breakthrough
0
2000
4000
6000
8000
10000
12000
14000
No BVs to 30% UV254 breakthrough

Figure 6f

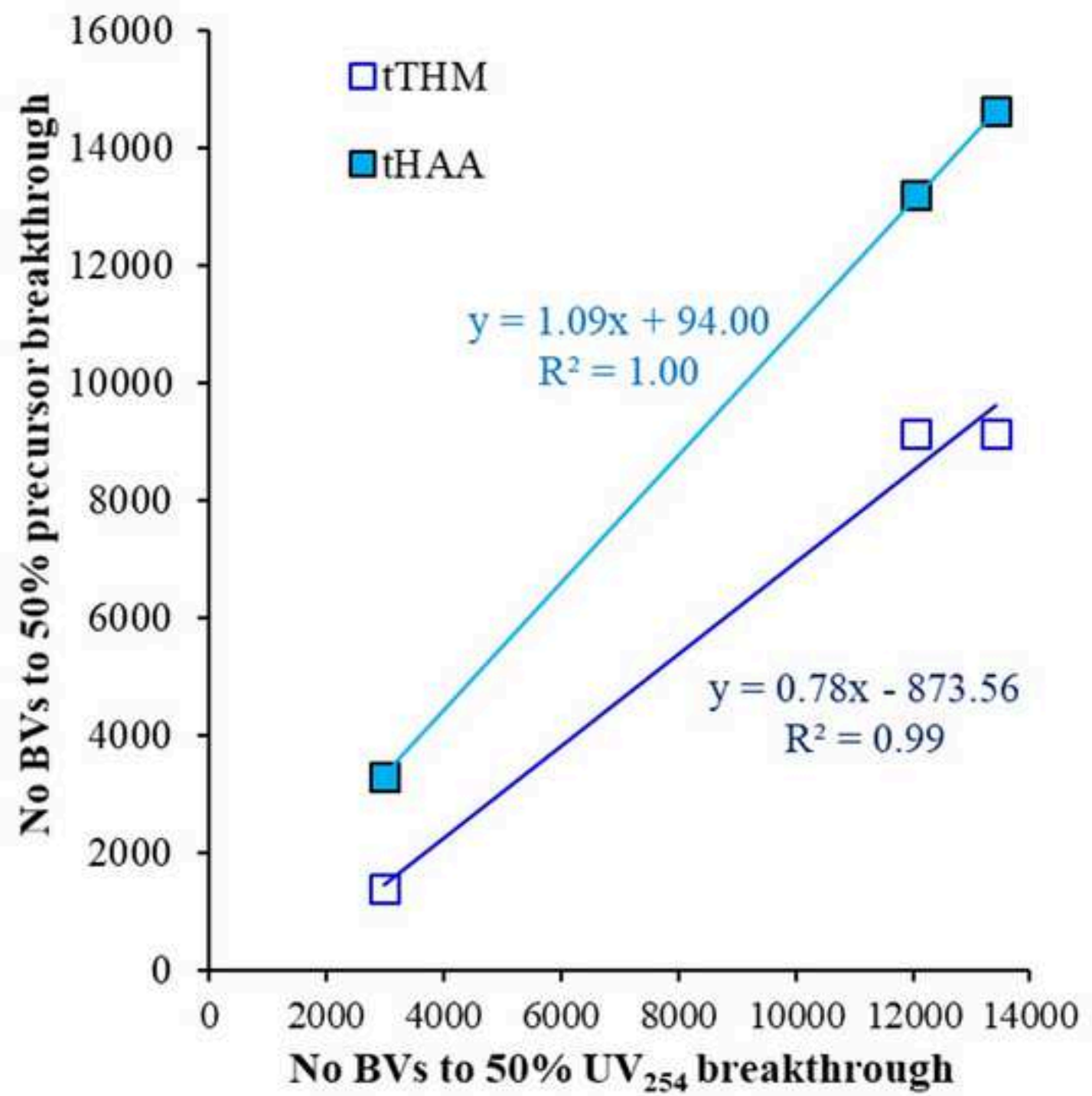
16000
14000
12000
10000
8000
6000
4000
2000
0
tTHM
tHAA
y = 1.09x + 94.00
R² = 1.00
y = 0.78x - 873.56
R² = 0.99
No BVs to 50% precursor breakthrough
0
2000
4000
6000
8000
10000
12000
14000
No BVs to 50% UV254 breakthrough

Figure 7a

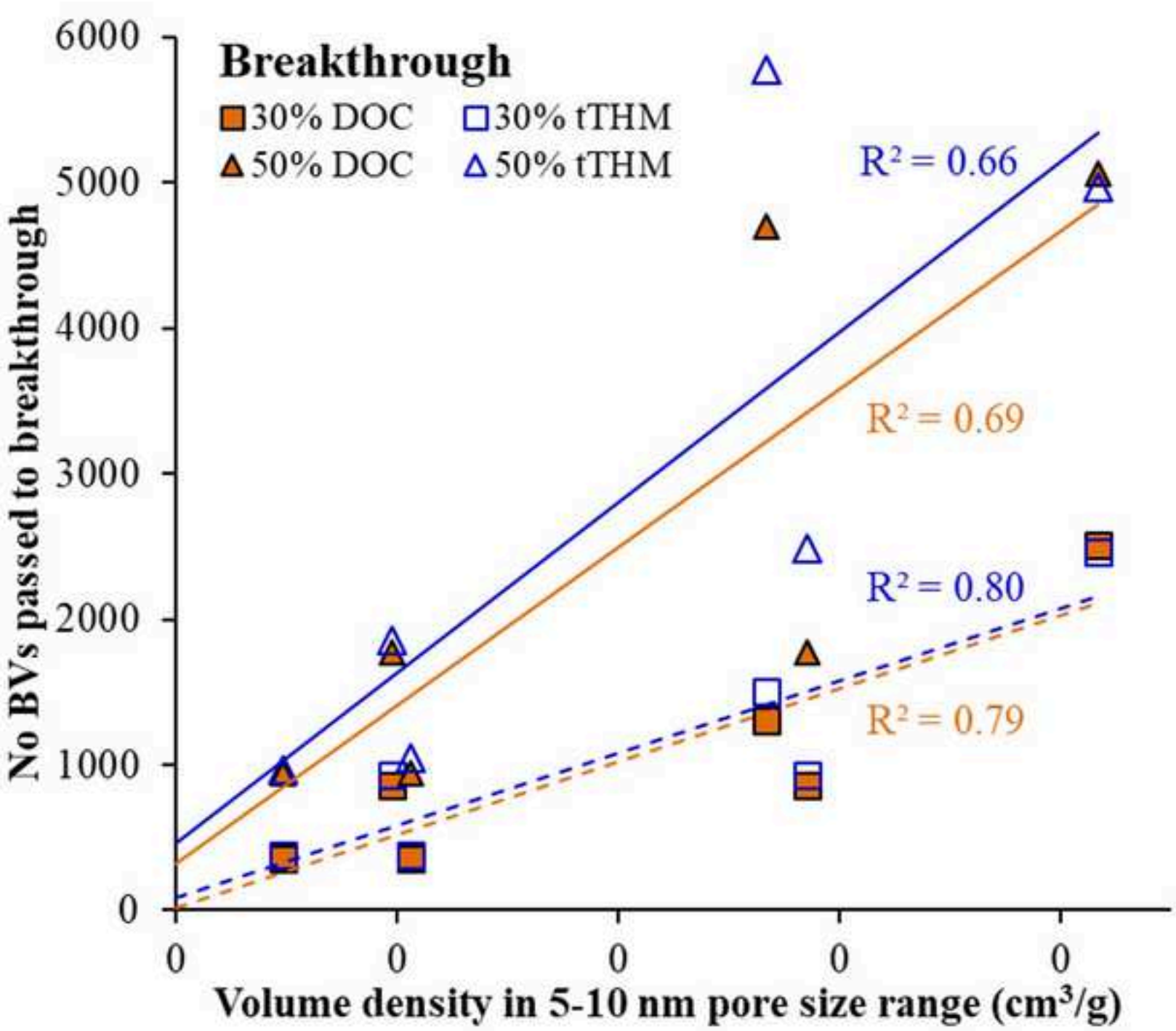
Breakthrough
30% DOC
30% tTHM
50% DOC
50% tTHM
R² = 0.66
R² = 0.69
R² = 0.80
R² = 0.79
No BVs passed to breakthrough
6000
5000
4000
3000
2000
1000
0
0
0
0
0
0
Volume density in 5-10 nm pore size range (cm³/g)

Figure 7b

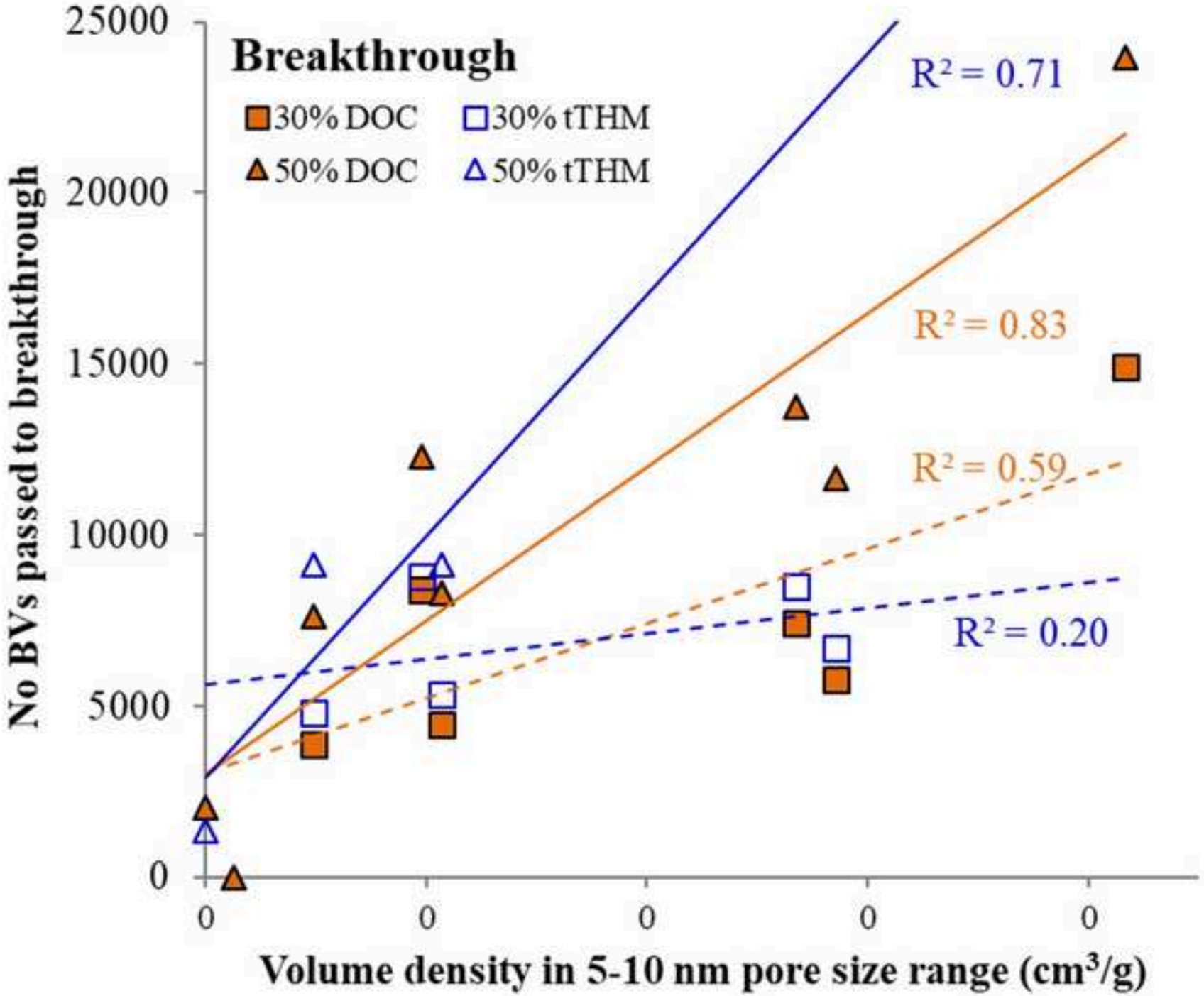
Breakthrough
30% DOC
30% tTHM
50% DOC
50% tTHM
R² = 0.71
R² = 0.83
R² = 0.59
R² = 0.20
No BVs passed to breakthrough
25000
20000
15000
10000
5000
0
0
0
0
0
0
Volume density in 5-10 nm pore size range (cm³/g)

Figure 7c

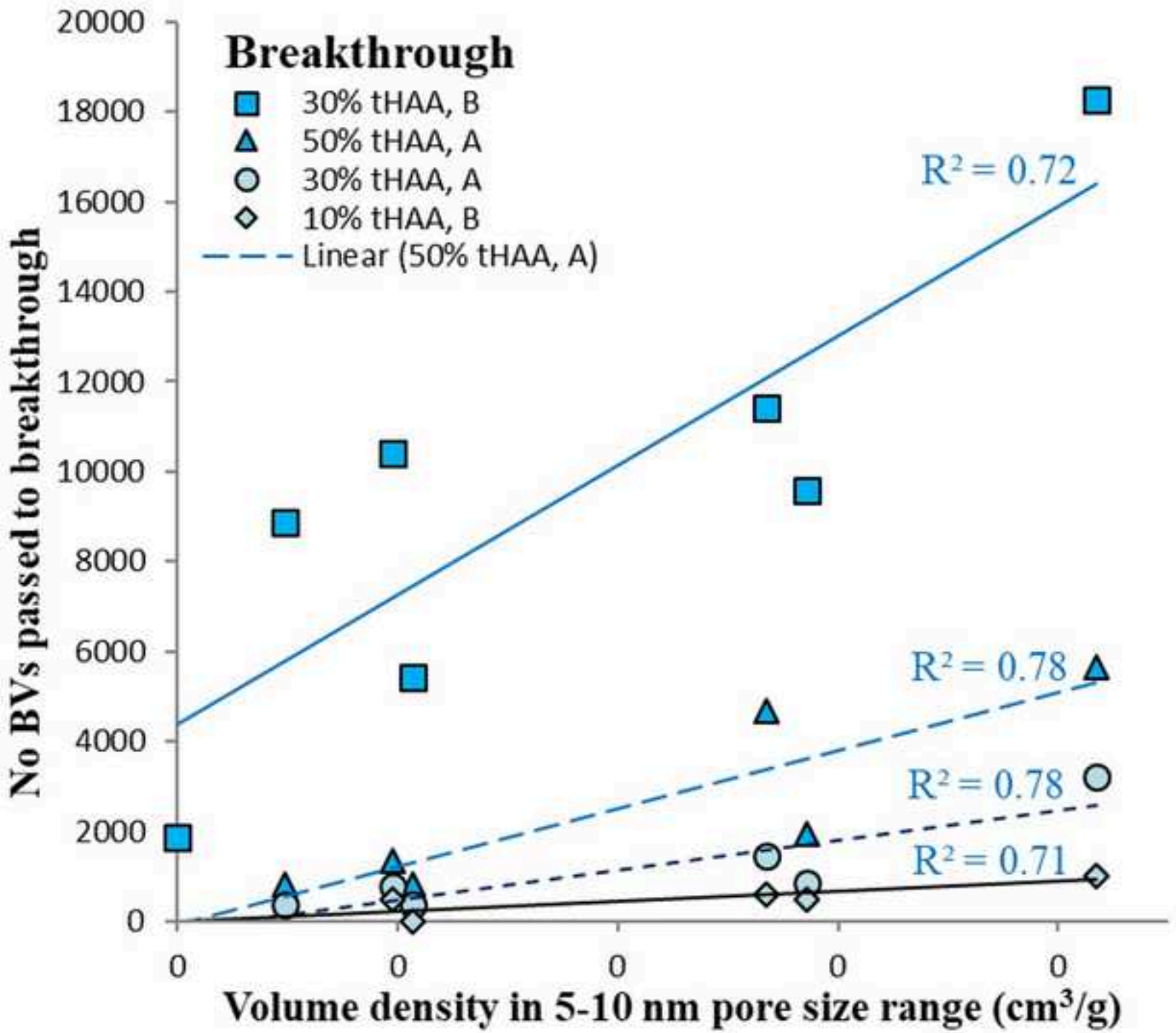
Breakthrough
30% tHAA, B
50% tHAA, A
30% tHAA, A
10% tHAA, B
Linear (50% tHAA, A)
R² = 0.72
R² = 0.78
R² = 0.78
R² = 0.71
No BVs passed to breakthrough
20000
18000
16000
14000
12000
10000
8000
6000
4000
2000
0
0
0
0
0
0
Volume density in 5-10 nm pore size range (cm³/g)

Figure 8

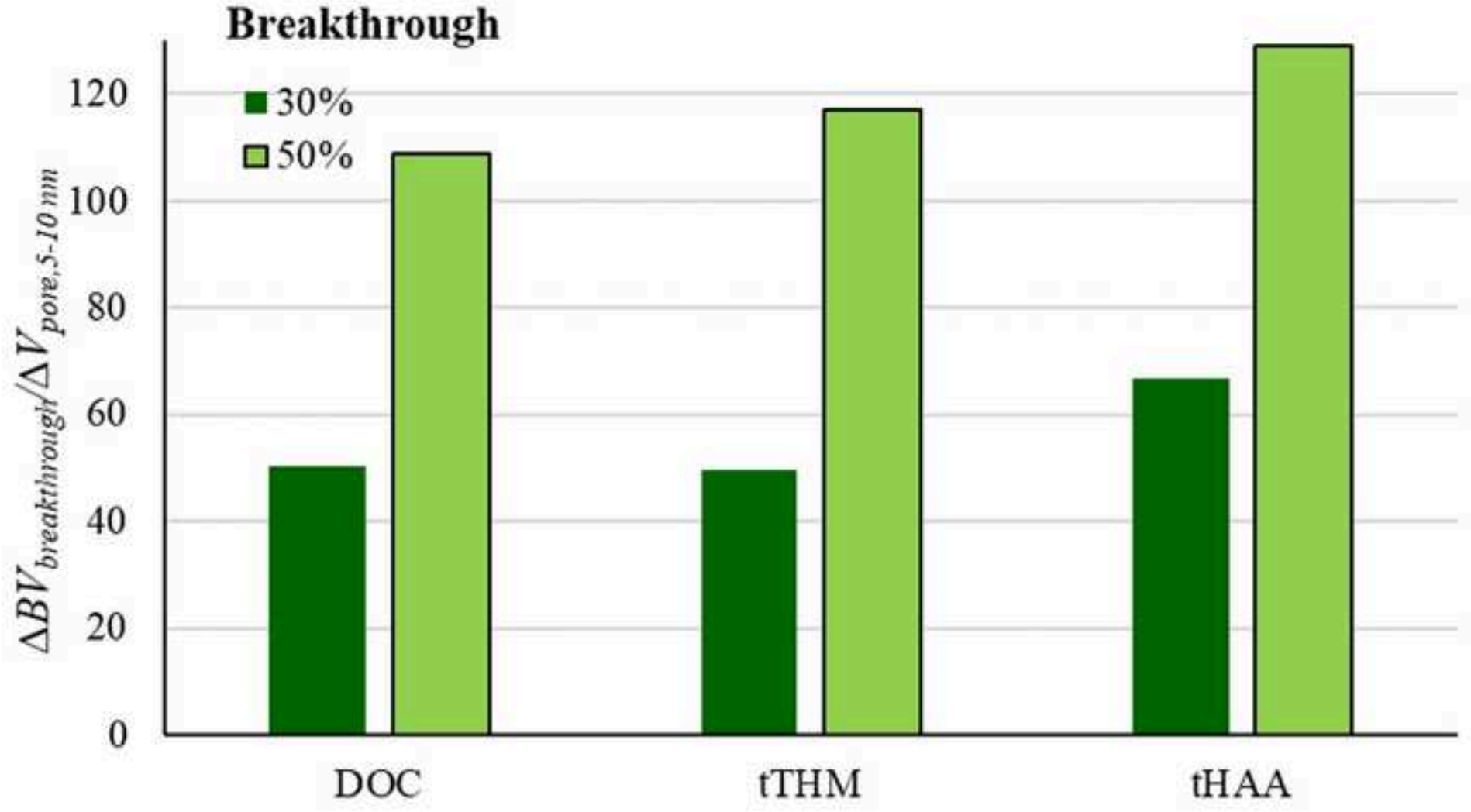
Breakthrough
30%
50%
120
100
80
60
40
20
0
$\Delta BV_{breakthrough}/\Delta V_{pore,5\text{-}10\,nm}$
DOC
tTHM
tHAA

**Table 1**

**Table 1:** Physicochemical characteristics of the two different water sources.

| *Parameter* | *Water A* | *Water B* |
|---|---|---|
| pH | 6.8 | 8.1 |
| DOC (mg/L) | 5.98 | 3.12 |
| $UV_{254}$ (/cm) | 0.254 | 0.068 |
| SUVA (mg/L/m) | 4.25 | 2.18 |
| tTHM (µg/L) | 676.3 | 282 |
| THMFP (µg/L per mg DOC) | 113.1 | 90.4 |
| tHAA (µg /L) | 1006.4 | 126 |
| $HAA_5FP$ (µg/L per mg DOC) | 168.3 | 40.4 |
| Colour (mg/L Pt/Co) | 33 | 4.47 |
| Turbidity (NTU) | 0.37 | 0.1 |
| Conductivity (µS/cm) | 166 | 569 |
| HPO (mg/L) | 3.44 | 1 |
| TPI (mg/L) | 1.25 | 0.71 |
| HPI (mg/L) | 0.37 | 1.05 |

**Table 2**
Click here to download Table: Table 2.docx

**Table 2:** The physicochemical properties of the media used for removal of NOM from two different water sources.

| *GAC media* | $V_{total}$ [1] cm³/g | $d_p$ nm | $V_{micropores}$ [2] cm³/g | $V_{meso-pores}$ [3] cm³/g | *DFT area ($m^2/g$)*[4] 0.7-1.7 | 1-2 | >2 | *Granulation*[5] mm | $S_{BET,s}$ [5] m²/g | $S_{BET}$ m²/g | *IN* [5,6] mg/g | *Precursor*[5] |
|---|---|---|---|---|---|---|---|---|---|---|---|---|
| *COL-L900* | 0.460 | ≤26.1 | 0.347 | 0.112 | 444 | 506 | 72 | 0.425-1.70 | 900-1000 | 977±5 | 900 | Bituminous coal |
| *F400* | 0.442 | ≤26.1 | 0.271 | 0.073 | 431 | 416 | 49 | 0.425-1.70 | 1050 | 1032±5 | 1050 | Bituminous coal |
| *208EA* | 0.517 | ≤16.1 | 0.301 | 0.120 | 424 | 465 | 67 | 0.6-1.7 | 1000 | 1078±6 | 1000 | Coal |
| *XC30* | 0.511 | ≤26.1 | 0.205 | 0.156 | 325 | 340 | 66 | 0.6-2.36 | 1000 | 986±6 | 950 | Coal |
| *DEO* | 0.331 | ≤27.3 | 0.174 | 0.013 | 274 | 285 | 8 | 0.6-1.70 | 800 | 809±11 | 825 | Coconut shell |
| *HT5* | 0.581 | ≤27.3 | 0.401 | 0.029 | 621 | 652 | 14 | 0.42-1.70 | 1400 | 1419±12 | 1300 | Coconut shell |
| *FY5* | 0.400 | ≤16.1 | 0.288 | 0.004 | 452 | 471 | 3 | 1.40-3.35 | 1150 | 1043±11 | 1100 | Coconut shell |
| *Brimac* | 0.430 | ≤25 | 0.246 | 0.131 | 334 | 373 | 62 | 0.7-2.38 | 200 | 841±3 | 700 | Bovine bones |

[1]According to DFT (density functional theory), determined to <30nm; [2]1-2 nm pore size range; [3]>2 nm pore size; [4]with reference to pore size range indicated; [5]Data sourced from supplier technical sheets; [6]Iodine number.

**Table 3**

Click here to download Table: Table 3.docx

**Table 3:** Volumetric pore size distribution, determined from DFT for pores sizes <30 nm.

| *Media/pore size:* | ***<0.7nm*** | ***0.7-5nm*** | ***5-10nm*** | ***10-15nm*** | ***15-20nm*** | ***20-25nm*** | ***25-30nm*** | ***Total*** |
|---|---|---|---|---|---|---|---|---|
| *Col-L900* | 0.001 | 0.440 | 0.011 | 0.006 | 0.002 | 0.001 | 0 | 0.460 |
| *F400* | 0.055 | 0.375 | 0.010 | 0.002 | 0 | 0 | 0 | 0.442 |
| *208EA* | 0.096 | 0.386 | 0.027 | 0.008 | 0.001 | 0 | 0 | 0.517 |
| *XC30* | 0.115 | 0.314 | 0.042 | 0.018 | 0.012 | 0.009 | 0.001 | 0.511 |
| *DEO* | 0.144 | 0.183 | 0.001 | 0.002 | 0.000 | 0 | 0 | 0.331 |
| *HT5* | 0.151 | 0.417 | 0.005 | 0.004 | 0.003 | 0.002 | 0 | 0.581 |
| *FY5* | 0.108 | 0.291 | 0 | 0.001 | 0 | 0 | 0 | 0.400 |
| *Brimac* | 0.053 | 0.316 | 0.029 | 0.016 | 0.010 | 0.007 | 0 | 0.430 |

**Table 4:** Throughput to a filtrate DOC of 30%, 50% and 80% of the feed concentration ($BV_{30}$, $BV_{50}$ and $BV_{80}$ respectively) for the GAC media studied by RSSCT, waters *A* and *B*, $EBCT_{LC}$ = 20 minutes.

| GAC media | WTW A | | | WTW B | | |
|---|---|---|---|---|---|---|
| | $BV_{30}$ | $BV_{50}$ | $BV_{80}$ | $BV_{30}$ | $BV_{50}$ | $BV_{80}$ |
| ***COL-L900*** | 355 | 946 | 10,710 | 4,467 | 8,284 | >>23,980 |
| ***F400*** | 858 | 1,775 | 10,030 | 8,402 | 12,308 | >>23,980 |
| ***208EA*** | 1,301 | 4,704 | >>22,194 | 7,455 | 13,728 | >>23,980 |
| ***XC30*** | 2,514 | 5,059 | >>22,194 | 14,911 | 23,964 | >>23,980 |
| ***DEO*** | <<267 | <<267 | 503 | <<1,302 | <<1,302 | 1,302 |
| ***HT5*** | 355 | 946 | 8,047 | 3,875 | 7,633 | >>23,980 |
| ***FY5*** | <<267 | <<267 | 1,242 | <<1,302 | 2,041 | 8,284 |
| ***Brimac*** | 858 | 1,775 | 17,101 | 5,798 | 11,657 | >>23,980 |

**Graphical Abstract**